The Plant Cell, Vol. 17, 1513–1531, May 2005, www.plantcell.org

Dynamics of COPII Vesicles and the Golgi Apparatus in Cultured *Nicotiana tabacum* BY-2 Cells Provides Evidence for Transient Association of Golgi Stacks with Endoplasmic Reticulum Exit Sites [W]

Yao-dong Yang,[a,1] Rabab Elamawi,[b,1] Julia Bubeck,[a] Rainer Pepperkok,[c] Christophe Ritzenthaler,[b] and David G. Robinson[a,2]

[a] Department of Cell Biology, Heidelberg Institute for Plant Sciences, University of Heidelberg, 69120 Heidelberg, Germany
[b] Institut de Biologie Moléculaire des Plantes, 67084 Strasbourg, France
[c] Cell Biology Cell Biophysics Programme, European Molecular Biology Laboratory, 69117 Heidelberg, Germany

Despite the ubiquitous presence of the COPI, COPII, and clathrin vesicle budding machineries in all eukaryotes, the organization of the secretory pathway in plants differs significantly from that in yeast and mammalian cells. Mobile Golgi stacks and the lack of both transitional endoplasmic reticulum (ER) and a distinct ER-to-Golgi intermediate compartment are the most prominent distinguishing morphological features of the early secretory pathway in plants. Although the formation of COPI vesicles at periphery of Golgi cisternae has been demonstrated in plants, exit from the ER has been difficult to visualize, and the spatial relationship of this event is now a matter of controversy. Using tobacco (*Nicotiana tabacum)* BY-2 cells, which represent a highly active secretory system, we have used two approaches to investigate the location and dynamics of COPII binding to the ER and the relationship of these ER exit sites (ERES) to the Golgi apparatus. On the one hand, we have identified endogenous COPII using affinity purified antisera generated against selected COPII-coat proteins (Sar1, Sec13, and Sec23); on the other hand, we have prepared a BY-2 cell line expressing Sec13:green fluorescent protein (GFP) to perform live cell imaging with red fluorescent protein–labeled ER or Golgi stacks. COPII binding to the ER in BY-2 cells is visualized as fluorescent punctate structures uniformly distributed over the surface of the ER, both after antibody staining as well as by Sec13:GFP expression. These structures are smaller and greatly outnumber the Golgi stacks. They are stationary, but have an extremely short half-life (<10 s). Without correlative imaging data on the export of membrane or lumenal ER cargo it was not possible to equate unequivocally these COPII binding loci with ERES. When a GDP-fixed Sar1 mutant is expressed, ER export is blocked and the visualization of COPII binding is perturbed. On the other hand, when secretion is inhibited by brefeldin A, COPII binding sites on the ER remain visible even after the Golgi apparatus has been lost. Live cell imaging in a confocal laser scanning microscope equipped with spinning disk optics allowed us to investigate the relationship between mobile Golgi stacks and COPII binding sites. As they move, Golgi stacks temporarily associated with COPII binding sites at their rims. Golgi stacks were visualized with their peripheries partially or fully occupied with COPII. In the latter case, Golgi stacks had the appearance of a COPII halo. Slow moving Golgi stacks tended to have more peripheral COPII than faster moving ones. However, some stationary Golgi stacks entirely lacking COPII were also observed. Our results indicate that, in a cell type with highly mobile Golgi stacks like tobacco BY-2, the Golgi apparatus is not continually linked to a single ERES. By contrast, Golgi stacks associate intermittently and sometimes concurrently with several ERES as they move.

INTRODUCTION

The endoplasmic reticulum (ER) is a highly versatile membrane compartment that extends throughout the cytoplasm of eukaryotic cells. Probably the most important of its numerous functions is that it acts as the port of entry for newly synthesized proteins that are destined for distribution and transport among the various organelles constituting the secretory and endocytic pathways. This characteristic feature was first established more than 30 years ago in classic studies on the intracellular transport of secretory proteins in mammalian cells (Palade, 1975) and has been continually elaborated on ever since (amongst numerous recent reviews, for animal cells, see Klumperman, 2000; Lee et al., 2004; for plants, see Jürgens, 2004; Ward and Brandizzi, 2004).

It is universally accepted that ER-to-Golgi protein transport in mammalian cells is mediated by the sequential action of COPII- and COPI-coat protein complexes (Duden, 2003; Lee et al., 2004). This is because a pleiomorphic structure known alternatively as the ER–Golgi intermediate compartment (ERGIC) and vesicular tubular clusters (VTCs) transits along microtubules

[1] These authors contributed equally to this work.
[2] To whom correspondence should be addressed. E-mail david.robinson@urz.uni-heidelberg.de; fax 49-6221-546406.
The author responsible for distribution of materials integral to the findings presented in this article in accordance with the policy described in the Instructions for Authors (www.plantcell.org) is: David G. Robinson (david.robinson@urz.uni-heidelberg.de).
[W] Online version contains Web-only data.
Article, publication date, and citation information can be found at www.plantcell.org/cgi/doi/10.1105/tpc.104.026757.

from the ER to the perinuclear-located Golgi apparatus with the help of a dynein/dynactin motor (Murshid and Presley, 2004). Characteristically, VTCs have COPI coats (Horstmann et al., 2002). However, there is general agreement that only the COPII machinery is responsible for the actual transport of cargo out of the ER (Barlowe, 1998, 2003).

In mammalian cells, export competent soluble and transmembrane cargo molecules collect at ER exit sites (ERES), which are defined by the presence of COPII-coat proteins, the ER-Golgi SNAREs Sed5, Bos1, Sec22, and Bet1, and several integral membrane proteins, including members of the p24 family and the Erv41/46 complex (Otte et al., 2001; Miller et al., 2002; Mossessova et al., 2003). The coat proteins are the GTPase Sar1p and two dimeric protein complexes: Sec23/24 and Sec13/31 at the cytosolic surface of the membrane (Antonny and Schekman, 2001). COPII-coat protein recruitment starts by the binding of Sar1p to the guanine nucleotide exchange factor (GEF) Sec12p, an integral ER membrane protein (Barlowe and Schekman, 1993), and is followed by the sequential attachment of Sec23/24 and then Sec13/31 dimers (Aridor and Balch, 2000). The Sec23/24 dimer has been implicated in the selection of cargo molecules into COPII vesicles (Bi et al., 2002; Miller et al., 2002) by interacting with diacidic (DXE) and diaromatic (FF) motifs in the cytoplasmic tails of transmembrane cargo molecules (Aridor et al., 2001; Otte and Barlowe, 2002).

In mammalian gland cells engaged in regulated secretion, ERES collect at specialized domains of the ER known as transitional ER (tER). Such domains are characterized by a high density of vesicle/tubule budding profiles in thin sections (for example, see Sesso et al., 1994; Bannykh et al., 1996; Ladinsky et al., 1999). The presence of COPII-coat proteins at these sites has been confirmed by immunogold labeling (Orci et al., 1991; Tang et al., 2000, 2001; Horstmann et al., 2002). tER is also often recognized in microorganisms. A clear example is that of the model alga *Chlamydomonas reinhardtii*, where tER and adjacent Golgi stacks are held in an ER amplexus attached to the nuclear envelope (Zhang and Robinson, 1986). Another well-known case is that of the fission yeast *Pichia pastoris*, which in contrast with *Saccharomyces cerevisiae* possesses a stacked Golgi apparatus (Mogelsvang et al., 2003). Pichia has several discrete tER domains each lying juxtaposed to a Golgi stack (Rossanese et al., 1999). The reason for such aggregations of COPII budding sites was thought to lie in the oligomerization status of Sec12p, which in *P. pastoris* has been shown to have large lumenal tails allowing for the interaction of adjacent molecules (Bevis et al., 2002). However, other scaffolding proteins, possibly Sec16p (Supek et al., 2002), now seem to be required for this event because COPII budding sites in *P. pastoris* still form when the localization of Sec12p to the tER is disrupted (Soderholm et al., 2004). In cultured cells and those mammalian cells exhibiting constitutive secretion, ERES are randomly located on the surface of the ER (Hammond and Glick, 2000; Stephens et al., 2000).

Like the yeasts, higher plant cells have a polydisperse Golgi apparatus and do not possess VTCs (Pavelka and Robinson, 2003). In addition, the Golgi apparatus moves along actin filaments that run parallel and close to the ER (Boevink et al., 1998; Ward and Brandizzi, 2004). Despite these clear morphological differences in the early secretory pathway, COPI/COPII vesiculating machineries appear to be quite conserved amongst the various eukaryotic cell types. Thus, COPI homologs can be found in the Arabidopsis database (Andreeva et al., 1998), and some have been identified in plant extracts (Movafeghi et al., 1999; Contreras et al., 2000, 2004). The presence of COPI proteins at the surface of vesicles budding from the periphery of Golgi cisternae has also been demonstrated by immunolabeling at both light (Ritzenthaler et al., 2002a) and electron microscopy levels (Pimpl et al., 2000). Many plant COPII homologs have also been detected and partially characterized (Sec12, Bar-Peled and Raikhel, 1997; Sar1 and Sec23, Movafeghi et al., 1999). Moreover, a functional Sar1 has been shown to be necessary for successful ER-to-Golgi transport in plant cells (Takeuchi et al., 2000; Phillipson et al., 2001).

tER in higher plant cells is poorly characterized, and vesiculation profiles at the ER in thin sections have only rarely been recorded in the literature (e.g., Craig and Staehelin, 1988; Staehelin, 1997; Ritzenthaler et al., 2002a), suggesting that ERES in this cell type are short lived and randomly distributed. To visualize ERES in tobacco (*Nicotiana tabacum*) BY-2 cells, we have employed two different approaches: (1) direct visualization of endogenous COPII proteins (Sar1, Sec13, and Sec23) by immunofluorescence microscopy in cell lines stably expressing ER- and Golgi-localized green fluorescent protein (GFP) markers and (2) visualization of ER-bound Sec13 by expression of a LeSec13:GFP construct in cells transiently expressing ER- and Golgi-localized red fluorescent protein (RFP) markers. In both cases, COPII is seen as punctate fluorescence over the surface of the ER. These point sources considerably outnumber Golgi stacks, although some are seen to associate with the rims of Golgi stacks. COPII labeling does not change or disappear with BFA, despite considerable morphological changes in the Golgi apparatus. Prevention of ER export through expression of a Sar1 mutant locked in the GDP state leads to disturbances in the ability to visualize COPII at the ER.

RESULTS

Generation of Plant COPII Antisera

We previously generated antibodies against an AtSec23 fragment (Movafeghi et al., 1999). To increase the certainty of valid identification of plant ERES by antibody labeling, we expressed fusion proteins and subsequently prepared and purified antibodies against two further COPII components: the GTPase AtSar1 and the coat protein AtSec13. Similarly, we prepared an antibody against AtSec12, the GEF required for Sar1 recruitment. We tested in protein gel blots all of these antibodies on membrane and cytosol fractions obtained from suspension cultured *Arabidopsis thaliana* and tobacco BY-2 cells (Figure 1A). With the exception of AtSec12, each antiserum recognized a single polypeptide in both subcellular fractions. This polypeptide corresponded to the expected molecular mass for the protein in question: 87 kD for AtSec23, 33 kD for AtSec13, and 22 kD for AtSar1. For AtSec12, a polypeptide of ~42 kD was detected only in the membrane fraction, as expected for a type I integral membrane protein (Bar-Peled and Raikhel, 1997).

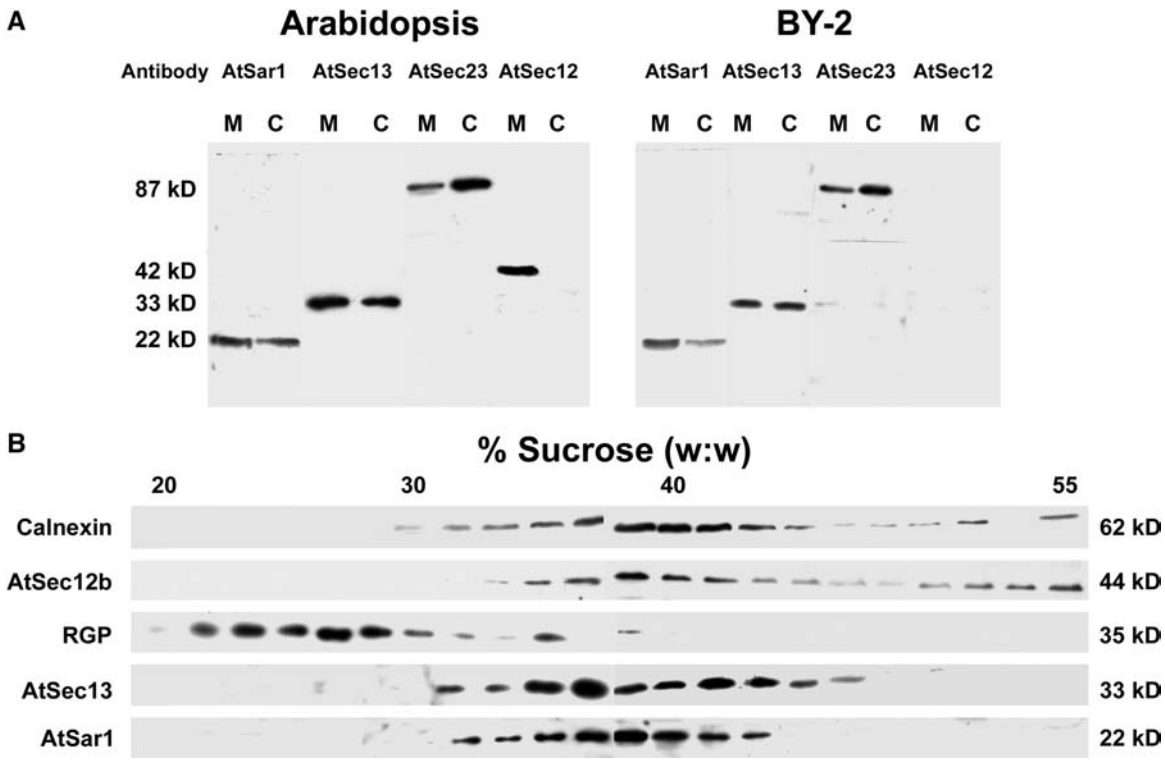

Figure 1. Cross-Reactivities of Antisera Raised against Recombinant Arabidopsis COPII Proteins.

(A) Cytosolic proteins and total membranes were isolated from the suspension cultures of Arabidopsis and tobacco BY-2 cells as described in Methods and probed with the antisera indicated. Equal amounts of protein were applied to the lanes in each gel blot (20 μg per lane for the Arabidopsis gel; 30 μg per lane for the BY-2 gel). M, membrane; C, cytosol.

(B) Arabidopsis total cell membranes separated on a linear isopycnic sucrose density gradient (as described in Methods). Individual fractions were probed with COPII antisera and with standard antisera for ER (calnexin) and Golgi (reversibly glycosylated polypeptide [RGP]) marker proteins.

Because our microscopy investigations were to be performed on BY-2 cells expressing various fluorescent ER and Golgi (X)FP constructs, we also prepared protein gel blots from fractions isolated from BY-2 cells. The same polypeptides were identified in both fractions; however, based on relative concentrations of applied proteins, the signals were estimated to be 40 to 50% weaker in the case of the BY-2 antigens. Interestingly, the AtSec12 antiserum consistently failed to cross-react with membrane preparations from BY-2 cells. Because a complete sequence for this protein from tobacco is not available, we cannot provide a reason for this.

We also tested the COPII antisera on fractions collected from a linear sucrose density gradient of Arabidopsis membranes to verify their association with the ER. As seen in Figure 1B, AtSec12, AtSec13, and AtSar1 have distribution profiles very similar to the ER marker calnexin and are clearly different to that of the Golgi marker reversibly glycosylated polypeptide. These results are consistent with our previous demonstration that the behavior of AtSec23-bearing membranes from cauliflower inflorescence in response to Mg^{2+} ions is typical for ER in sucrose gradients.

COPII Immunostaining in Tobacco BY-2 Cell Lines Expressing Fluorescent ER and Golgi Markers

Immunofluorescence labeling of wild-type and transgenic BY-2 cells with COPII antisera gave rise in all cases to a punctate pattern (Figure 2). A similar picture was produced with all three antisera: anti-AtSec23 (Figures 2A and 2K), anti-AtSec13 (Figure 2B), and anti-AtSar1 (Figures 2E, 2H, and 2M). The signal density was lower in median sections (Figures 2A to 2C) than in optical sections through the cell cortex parallel to the cell surface (Figures 2D to 2M), presumably because of the higher incidence of ER in surface view. Colocalization of labeling when using any two of the three COPII antisera lay regularly between 50 and 60%.

In BY-2 cells expressing the Golgi marker GmMan1:GFP, immunostaining with anti-AtSar1 gave rise to a homogeneous punctate image in cortical optical sections (Figures 2D to 2F). The density of this labeling was found to be 3.9, 4.4, and 3.5 point sources/μm^2 in Figures 2F, 2I, and 2L, respectively, with diameters of 540 $\pm$ 174 nm, 568 $\pm$ 230 nm, and 512 $\pm$ 166 nm ($n >$ 100), respectively. By comparison, Golgi stacks with an average apparent diameter of 880 $\pm$ 164 nm ($n = 77$) had a density of only

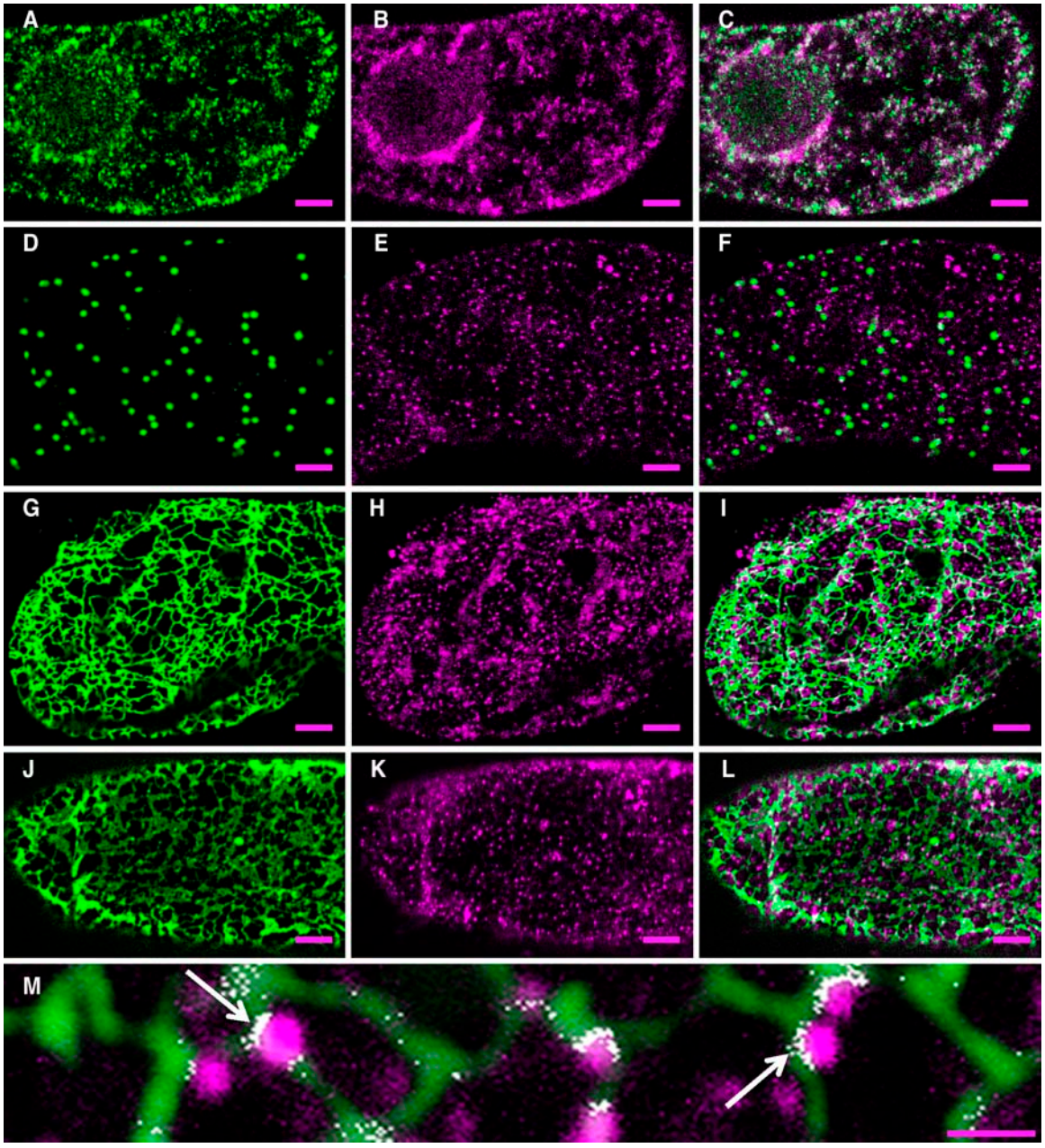

Figure 2. Confocal Immunofluorescence Images of BY-2 Cells Labeled with AtCOPII Antisera.

(A) Anti-AtSec23 staining.
(B) Anti-AtSec13 staining.
(C) Merge image of **(A)** and **(B)**; median optical section, wild-type cell.
(D) Golgi stacks visualized in a GmMan1:GFP transformed cell; cortical section.
(E) Anti-AtSar1 staining of cell in **(D)**.
(F) Merge image of **(D)** and **(E)**.
(G) Cortical ER visualized in a GFP:HDEL transformed cell.
(H) Anti-AtSar1 staining of cell in **(G)**.
(I) Merge image of **(G)** and **(H)**.
(J) Cortical ER in GFP:HDEL transformed cell.
(K) Anti-AtSec13 staining of cell in **(J)**.
(L) Merge image of **(J)** and **(K)**.
(M) High magnification of cortical ER (green, GFP:HDEL) with COPII visualized with anti-AtSar1 (red; colocalization indicated in yellow).
Bars = 5 μm for all panels except **(M)** (1 μm).

1.5/μm^2 (Figure 2F). COPII antibody staining did not appear to be preferentially associated with cisternae of the cortical ER network (Figures 2G to 2L). At high magnifications, individual punctate COPII fluorescent signals were often found sitting directly on strands of ER (see arrows in Figure 2M). Using the same parameters for the estimations obtained from Figure 2F, the average diameter of these signals was 456 $\pm$ 18 nm ($n = 43$). Interestingly, and in agreement with immunostaining for COPII in mammalian cells (Rust et al., 2001), the colocalization (yellow) of green (GFP:HDEL) and red (anti-AtSar1) signals is restricted to narrow semicircular profiles on the ER. Punctate fluorescent signals of a similar size were also seen lying adjacent to the ER tubules. These could represent either ER-bound COPII out of the plane of section or individual released COPII vesicles, as suggested by Rust et al. (2001).

Establishment of a Tobacco BY-2 Cell Line Expressing LeSec13:GFP

To visualize and study the dynamics of ERES in living cells, we transformed BY-2 cells with *Lycopersicon esculentum* (Le)-Sec13:GFP. To minimize potential toxic side effects related to LeSec13-GFP overproduction, an inducible promoter system was preferred to a 35S stable expression system for BY-2 transformation. However, to rule out the possibility that the expression of this construct might influence the manifestation of ERES, for example, by enhancing secretory activity through an increased number of ERES, we examined the effects of the Sec13:GFP construct on the secretory index (ratio of extracellular to intracellular activities of a secretory enzyme; Phillipson et al., 2001). To do this, we electroporated tobacco mesophyll protoplasts with constant amounts of plasmid encoding for α-amylase together with increasing amounts of Sec13:GFP plasmid DNA. As shown in Figure 3, Sec13:GFP had no effect on the secretion index, even at high concentrations of plasmid DNA. As a control we also tested Sar1[H74L], a mutated form of Sar1 fixed in the GTP form. In agreement with the results of daSilva et al. (2004), this mutant proved to be a potent inhibitor of secretion. Thus, it would appear that the secretory pathway in tobacco is not influenced by the overexpression of (X)FP-tagged COPII-coat proteins (here, Sec13, and Sar1 in daSilva et al., 2004).

Beginning ~24 h after exposure to dexamethasone, the BY-2 cells were expressing the Sec13:GFP fusion construct in sufficient quantities to allow for detection by confocal microscopy. In optical sections taken through the cortex (Figure 4A), a dense punctate image was obtained, similar to the antibody staining generated with COPII antisera (Figure 2). When cells expressing the GFP fusion construct were fixed and immunostained with AtSec13 antibodies, almost a perfect colocalization was obtained (Figures 4B to 4D), confirming the Sec13 identity of the protein carrying the GFP signal. During cytokinesis, the LeSec13:GFP signal in mitotic BY-2 cells is clearly seen to aggregate in and around the phragmoplast (Figure 4E), a region in which Golgi stacks are excluded (Figures 4H and 4I). Interestingly, when the LeSec13:GFP signal is compared with that of coexpressed BiP:DsRed (immunoglobulin binding protein cognate, a lumenal marker of the ER), there are discrete differences in the distribution of the two (Figures 4F and 4G). Although there is a clear colocalization of the two fluorescent signals in the phragmoplast, BiP:DsRed is absent from the reformed nuclear envelope. In contrast with LeSec13:GFP, BiP:DsRed is localized to the division plane, suggesting that the ER that gets trapped in the plasmodesmata of the cell plate lacks the capacity to bind COPII.

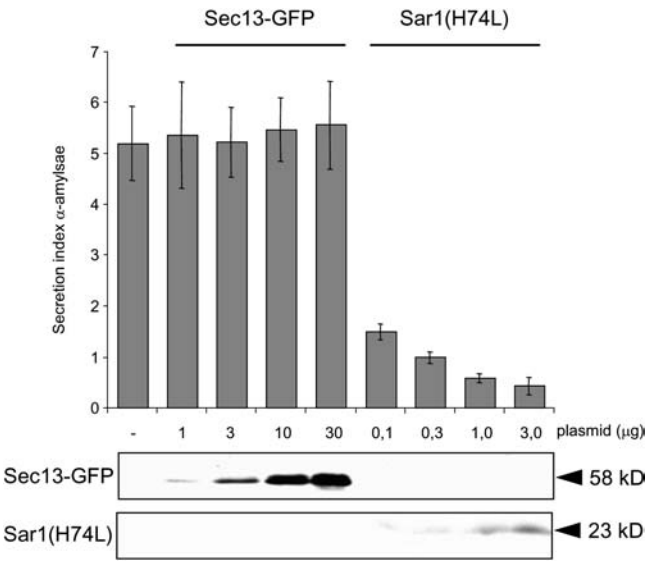

Figure 3. Expression of Sec13-GFP Is without Effect on Secretion.

Tobacco protoplasts were electroporated with a constant amount of plasmid encoding for α-amylase together with increasing amounts of plasmid encoding for LeSec13-GFP or for the GTP-blocked mutant Sar1[H74L]. Standard deviations, as indicated by error bars, were calculated from six separate experiments. Protein gel blots of total cytosolic proteins, corresponding to the individual panels of the secretion index histogram, are also given to document the gradual increase in expressed effector protein in the protoplast homogenates. Note that in marked contrast with LeSec13-GFP, the expression of the Sar1 mutant leads to a drastic reduction in secretory activity.

Median optical sections from BY-2 cells expressing LeSec13:GFP reveal, in addition to punctate fluorescence throughout the cytoplasm, an intense staining of the nuclear envelope and a diffuse staining of the nuclear matrix except for the nucleoli (Figure 4J). This, for us initially unexpected result, is fully in keeping with the known behavior of Sec13 in other eukaryotic cells. In yeast, it has been shown that, in addition to being a COPII-coat protein, Sec13p is also incorporated into the nuclear pore complex Nup84p (Siniossoglou et al., 2000). Moreover, in mammalian cells, Sec13 has recently been shown to shuttle between the cytosol and nuclear matrix (Enninga et al., 2003). As shown in Figure 5, we have performed on the LeSec13:GFP BY-2 cell line the same kind of fluorescence recovery after photobleaching (FRAP) experiments that were performed by the latter authors. Recovery of LeSec13:GFP at the nuclear rim was still not observed after 60 min when a region of the nuclear envelope that also included part of the ER, cytosol, and nuclear matrix was photobleached (Figures 5D and 5F). By contrast, the pool of cytosolic and ER-associated LeSec13:GFP recovered very rapidly (Figure 5C). When most of the area of the nucleus was photobleached, a near complete recovery of

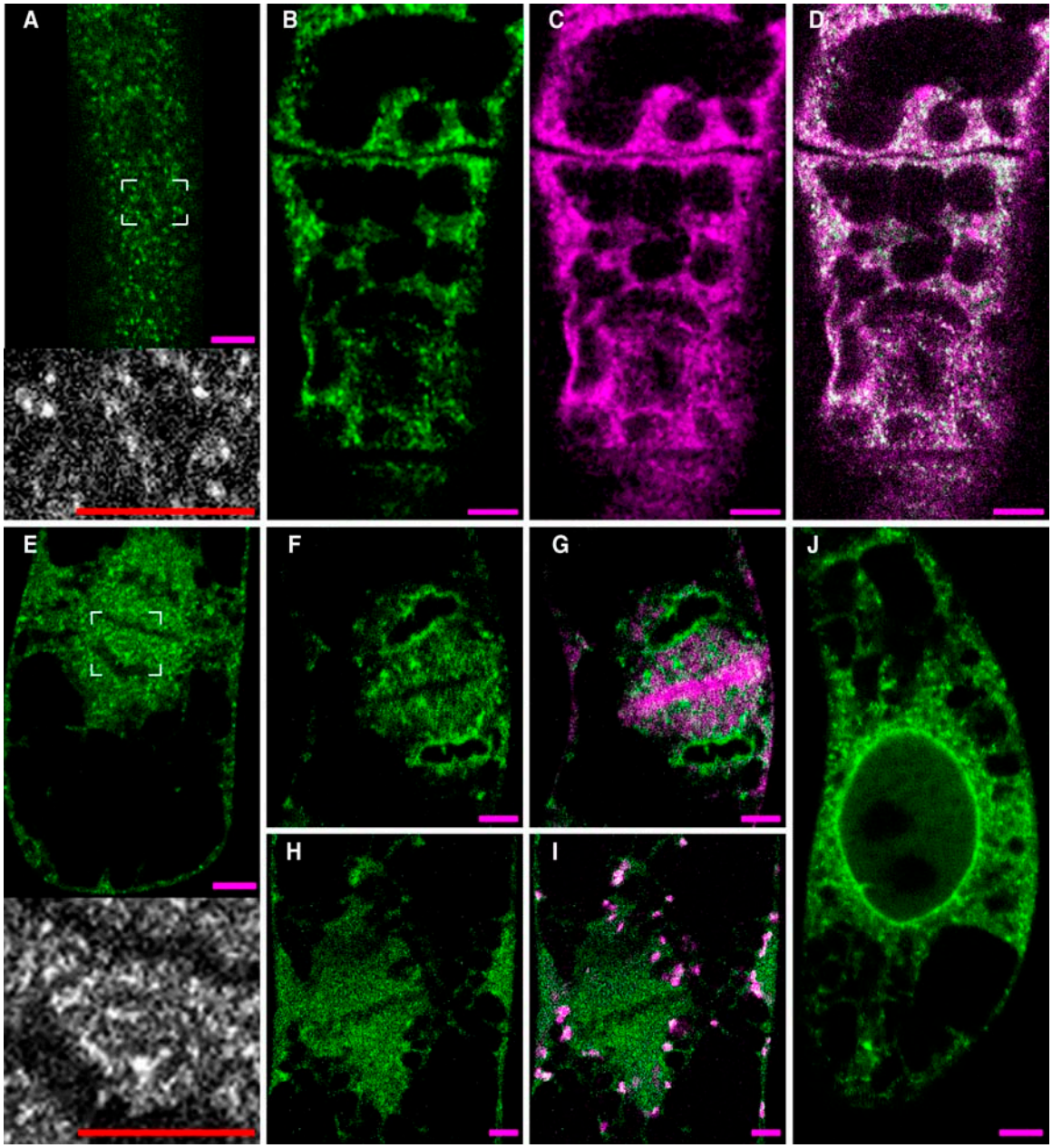

Figure 4. Visualization of COPII in BY-2 Cells Expressing AtSec13:GFP.

(A) Punctate GFP signal in cell cortex. Inset is a high magnification.
(B) to **(D)** Antibody staining of AtSec13 in LeSec13:GFP cell line; GFP signal **(B)**, immunofluorescence labeling **(C)**, merged image **(D)**.
(E) LeSec13:GFP fluorescence pattern in a mitotic cell (late anaphase). Inset is high magnification of area indicated in brackets.
(F) and **(G)** As for **(E)** but for telophase. **(F)**, LeSec13:GFP fluorescence; **(G)**, as for **(F)** but revealing coexpressed BiP:DsRed.
(H) and **(I)** Distribution of Golgi stacks during mitosis. **(H)**, LeSec13 fluorescence; **(I)**, Golgi stacks revealed by expression of GmManI-RFP.
(J) Median optical section revealing a distinct staining of the nuclear envelope and nuclear matrix, in addition to punctate signals in the cytoplasm.
Bars = 5 μm.

intranuclear LeSec13:GFP was detected after 10 min with a half-time of ~2 min (Figures 4G to 4J). This was significantly slower than the recovery of free GFP (half-time of 30 s). These results suggest a very rapid exchange of LeSec13:GFP molecules between the cytoplasm and the ER, a slower exchange between the nucleus and the cytoplasm, and a high stability of the nuclear pore complex-bound LeSec13:GFP. More importantly, they are almost identical to those obtained by Enninga et al. (2003), underlining yet again the credibility of the fluorescence signal we obtained with the LeSec13:GFP construct.

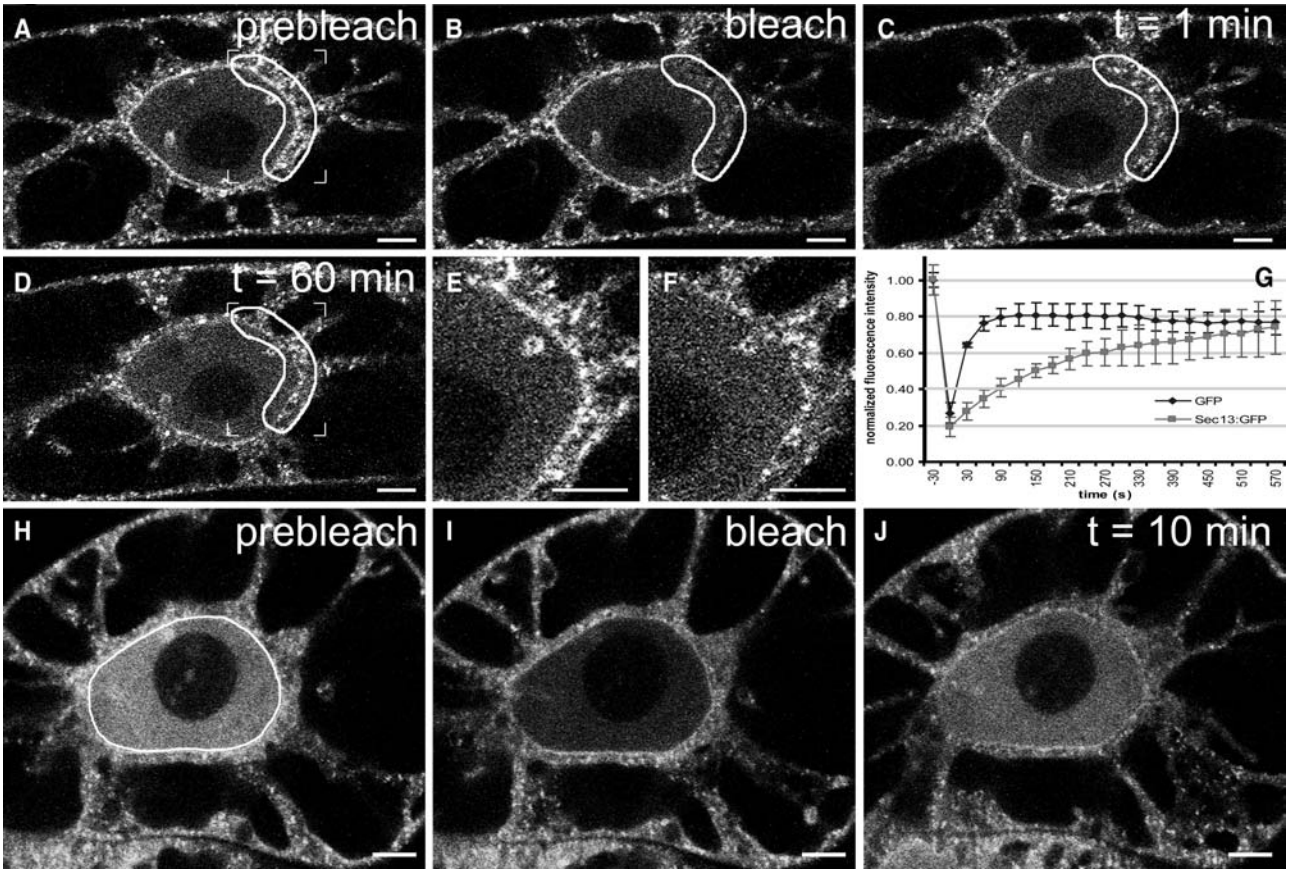

Figure 5. Analysis of LeSec13:GFP Dynamic by FRAP.

(A) to **(D)** FRAP analysis of LeSec13:GFP present within the nuclear envelope, ER, and cytosol. LeSec13:GFP fluorescence was monitored before **(A)**, immediately after photobleaching **(B)**, as well as 1 min **(C)** and 60 min **(D)** after recovery.

(E) and **(F)** Detailed views of the boxed regions shown in **(A)** and **(D)**, respectively.

(G) to **(J)** FRAP analysis of nuclear LeSec13:GFP.

(G) Plots show fluorescence recovery of nuclear LeSec13:GFP versus free GFP in the bleached area. Images were acquired every 30 s. Measurements of fluorescence intensity were subtracted from background fluorescence and normalized from loss of fluorescence during bleaching and imaging. Error bars are standard deviations ($n = 3$).

(H) to **(J)** The images show single optical sections of LeSec13:GFP present within the nucleus before **(H)** and immediately after photobleaching **(I)** as well as 10 min after recovery **(J)**. Bleached areas are circled in white.

Bars = 5 μm.

To gain further insights into the dynamics of the LeSec13:GFP fluorescence, LeSec13:GFP expressing cells were visualized by time-lapse microscopy (Figure 6). Because of the rapidity at which the fluorescent points appear and disappear, Nipkov disk–based confocal microscopy proved superior to conventional confocal laser scanning microscopy for this analysis. With this imaging technique we were able to continuously observe changes in cortical LeSec13:GFP for several minutes without any apparent photobleaching (Figure 6; see Supplemental Video 1 online). Taken separately, individual frames appeared very similar to the images obtained with fixed cells (cf. Figures 5 and 4A): numerous punctate fluorescent structures that averaged 430 ± 220 nm ($n > 900$) in diameter with a density of 5.0 punctate structures·μm^{-2} were observed. A comparison between successive frames revealed that only very few point light sources could be followed for any significant length of time, making an estimation of their movement impossible. Thus, on successive frames (arrowheads and circles, Figure 6A), the point light sources appeared immobile. We therefore conclude that COPII binding has a very short half-life (at the most 10 s). This results in a blinking rather than moving appearance of LeSec13:GFP fluorescence.

Effects of Secretory Inhibitors on COPII Immunostaining and LeSec13:GFP Fluorescence

The physiological relevance of the COPII visualizations described above can be tested by analyzing the effects of substances known to perturb the secretory pathway. Because the dependency of ER export on Sar1-GTP had already been

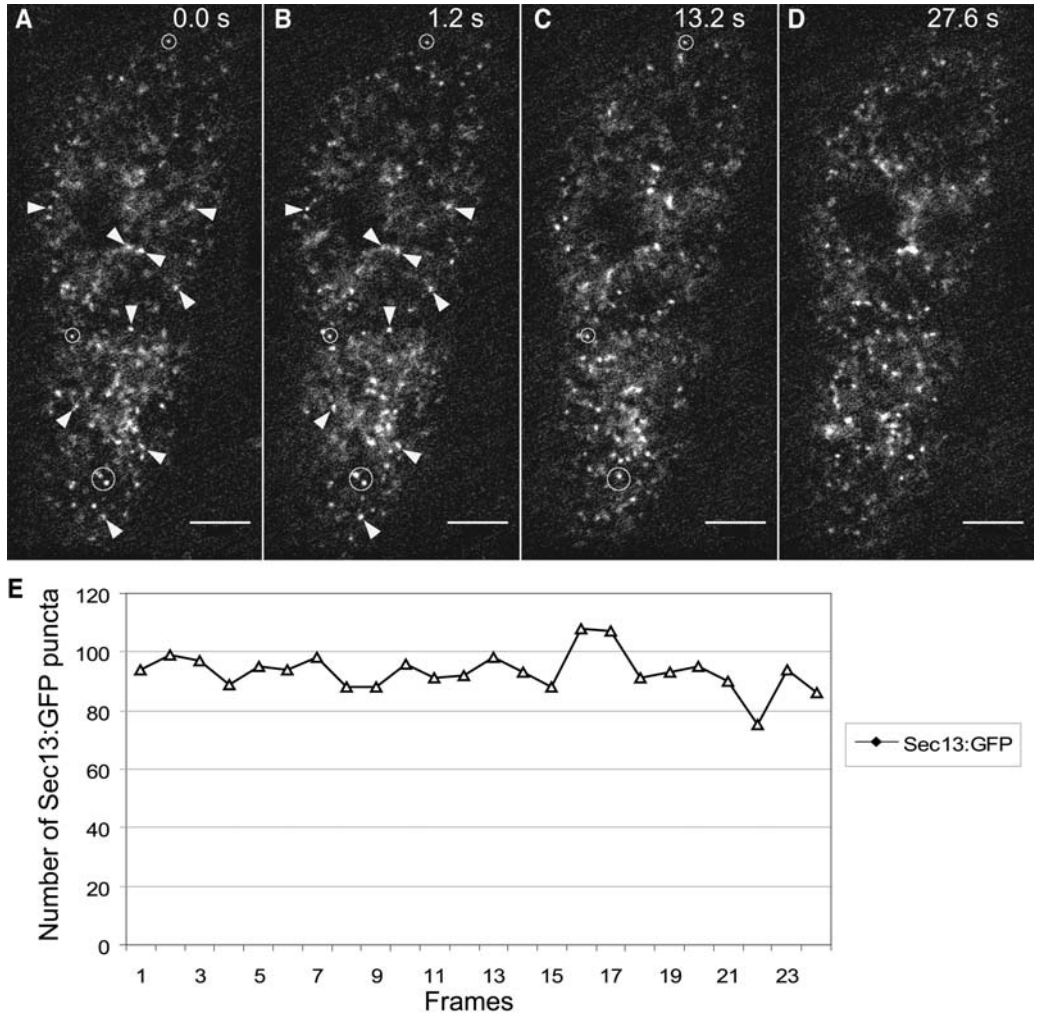

Figure 6. Analysis of LeSec13:GFP Dynamic by Time-Lapse Microscopy.

(A) to **(D)** Cortical LeSec13:GFP was visualized using an Ultra*VIEW* RS confocal microscope. Single optical sections images were acquired every 1.2 s for 27.6 s (see Supplemental Video 1 online). Images taken at 0, 1.2, 13.2, and 27.6 s are presented (**[A]** to **[D]**, respectively). Arrowheads and circles indicate LeSec13:GFP punctate structures that remained immobile for at least 1.2 and 13.2 s, respectively. Bars = 5 μm.

(E) Number of fluorescent foci in each individual frames of the video were calculated using the analyze particles command in ImageJ and were plotted on a graph.

established (Takeuchi et al., 2000; Phillipson et al., 2001), we decided to examine the consequences of expression of Sar1[T39N], a mutated form of Sar1 fixed in the GDP form. To confirm that Sar1[T39N] blocks secretion in BY-2 cells, we coexpressed a secretory form of RFP (SP:RFP). In control cells, SP:RFP is secreted into the membrane but also accumulates in the vacuole (Figures 7A to 7C). When Sar1[T39N] is expressed, SP:RFP is retained in the ER (Figures 7D to 7F). Under these conditions, a smeared rather than a clear punctate image for LeSec13:GFP fluorescence was observed (Figures 7G to 7J). We attribute this imperfect COPII image to impaired recruitment of Sec13/23 as a result of insufficient Sar1-GTP.

The macrocyclic lactone brefeldin A (BFA) is often used to block secretion (reviewed in Nebenführ et al., 2002). In addition to perturbing the Golgi apparatus, it has been suggested that BFA might also directly affect ER export (Brandizzi et al., 2002). This claim has recently found support in the observation that the distribution of punctate Sar1-YFP structures on the ER of tobacco epidermis is changed upon addition of BFA (daSilva et al., 2004). We therefore decided to investigate what effects BFA has on the COPII structures we have visualized in BY-2 cells by applying the drug to the LeSec13:GFP cell line expressing the *cis*-Golgi marker GmManI-RFP. Treatment with 10 $\mu g \cdot mL^{-1}$ lead to a complete redistribution of the RFP-tagged protein into the ER but appeared to have no effect on the LeSec13:GFP punctate structures (Figures 8A to 8F). Similarly, BFA had no effect on COPII visualization when performed by immunostaining with AtSec13 antibodies (Figures 8G to 8I).

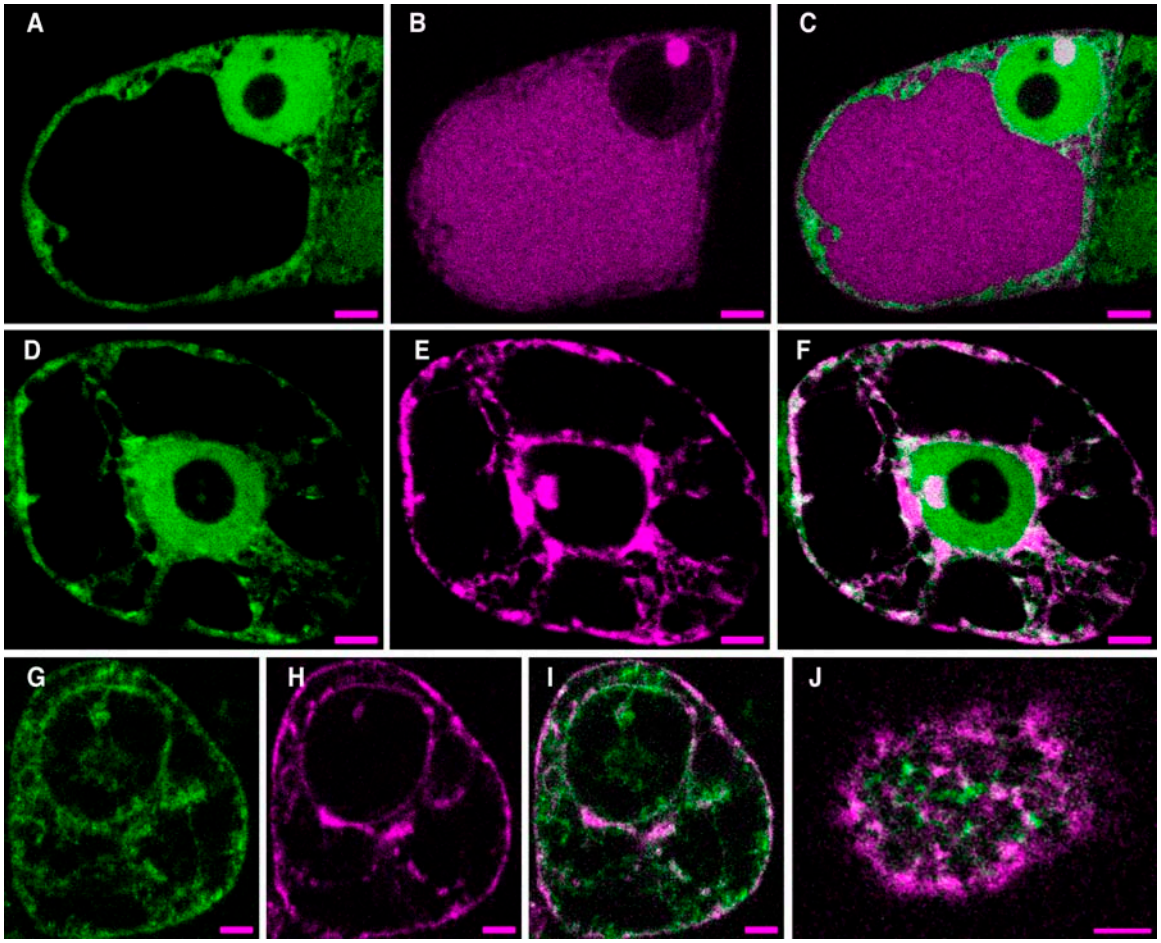

Figure 7. Effects of Sar1[T39N] Secretory Inhibitors on LeSec13:GFP.

(A) to **(F)** LeSec13:GFP-expressing cells were transformed by biolistics so as to express SP:RFP alone (**[A]** to **[C]**) or together with Sar1[T39N] (**[D]** to **[F]**). LeSec13:GFP distribution (**[A]** and **[D]**); SP:RFP distribution (**[B]** and **[E]**). Note that SP:RFP is vacuolar in the absence of Sar1[T39N] **(B)** and is retained in the ER upon Sar1[T39N] expression **(E)**. **(C)** and **(F)** are merged images corresponding to **(A)** and **(B)** and **(D)** and **(E)**, respectively.
(G) to **(J)** Effect of Sar1[T39N] in cells coexpressing LeSec13:GFP and GmManI-RFP. LeSec13:GFP signal **(G)**; GmManI:RFP signal **(H)**. Note that GmManI:RFP is redistributed into the ER. **(I)** and **(J)** are merged images showing a median **(I)** and a cortical single optical section **(J)**.
Bars = 5 μm.

Sec13:GFP Fluorescence in Relation to the ER and Golgi in Living BY-2 Cells

Simultaneous fluorescence imaging of the ER and Golgi apparatus in cells expressing LeSec13:GFP is possible when these organelles are made visible with YFP or RFP constructs. We therefore prepared BiP:DsRed and GmMan1:RFP as ER and Golgi markers, respectively. The validity of BiP:DsRed as an ER marker was confirmed by bombarding transgenic BY-2 cells expressing GFP:HDEL. The typical cortical ER network was revealed by both fluorescent markers and showed complete colocalization (data not shown). An identical image was also obtained when BY-2 cells transiently expressed Sec12-YFP, the GEF for Sar1 (Figures 9A to 9C). When the inducible LeSec13:GFP cell line was bombarded with BiP:DsRed, the punctate green COPII coats were highlighted against the tubular red ER network (Figures 9D to 9F). However, as was the case with the immunostaining for COPII-coat proteins (see Figures 2G to 2M), many of the LeSec13:GFP punctate signals lay adjacent to the ER tubules.

To confirm the validity of GmMan1-RFP as a Golgi marker, we bombarded transgenic BY-2 cells expressing GmMan1:GFP with GmMan1-RFP. Again, a perfect colocalization with both Golgi markers was obtained (data not shown). The LeSec13:GFP cell line was then bombarded with GmMan1-RFP. Optical sections in the cortical region of a cell are presented in Figures 9G and 9H . As with the antibody staining data presented above, the LeSec13:GFP fluorescent points greatly outnumbered the Golgi stacks (Figure 9I). However, some of the Golgi stacks were densely surrounded at their periphery by LeSec13:GFP fluorescence, giving rise to a kind of halo (see the group of Golgi stacks in the middle of Figure 9I, and Figure 9K), whereas others were relatively free (Figure 9J).

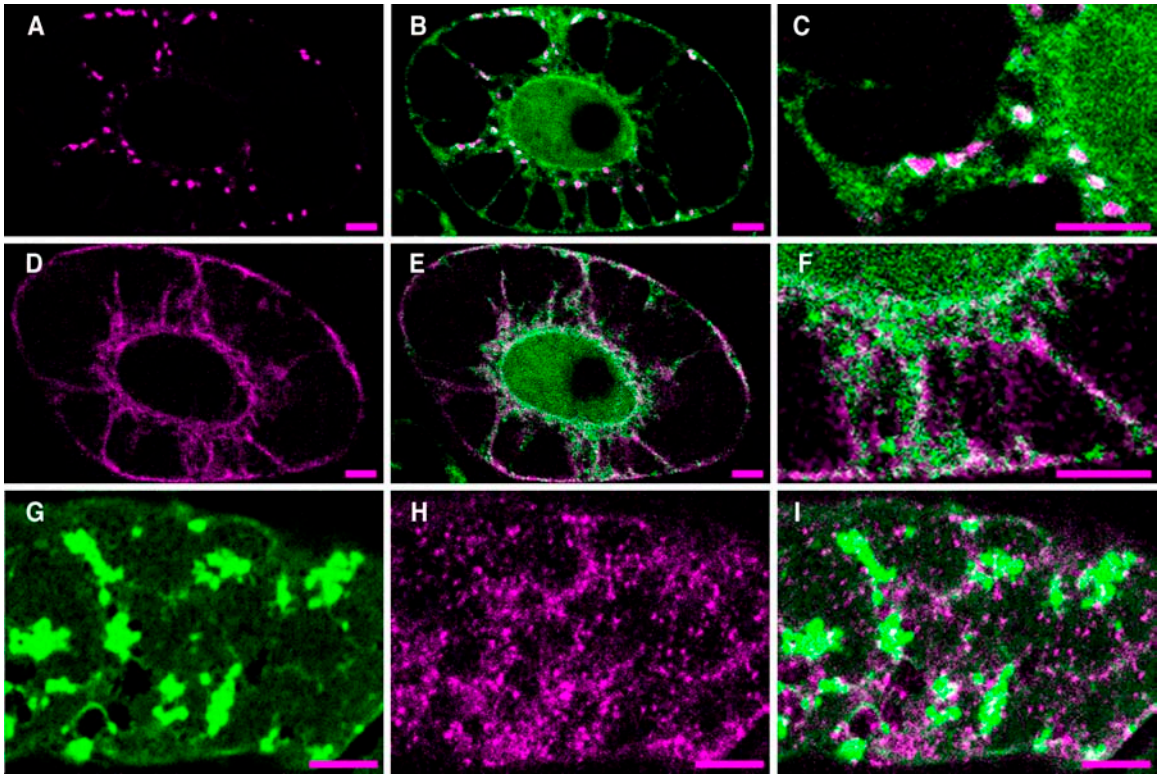

Figure 8. Effect of BFA on LeSec13:GFP.

(A) to **(F)** LeSec13:GFP cells were transformed by biolistics so as to coexpress GmManI:RFP and were monitored before (**[A]** to **[C]**) and after a 20-min treatment with 10 $\mu g \cdot L^{-1}$ BFA (**[D]** to **[F]**). BFA treatment led to the complete redistribution of GmManI:RFP from the Golgi **(A)** into the ER **(D)**. Covisualization of LeSec13:GFP (green) and GmManI:RFP (red) at low magnification and high magnification is shown in **(B)** and **(E)** and **(C)** and **(F)**, respectively.

(G) to **(I)** Immunodetection of Sec13 in GmMan1:GFP cells treated for 60 min with BFA. GmMan1:GFP signal **(G)**; anti-AtSec13 immunolabeling **(H)**; corresponding merged image **(I)**.

Bars = 5 μm.

COPII Associates with Mobile Golgi Stacks at Their Rims

To analyze the relationship between COPII and Golgi stacks at greater resolution, we have observed live BY-2 cells expressing LeSec13:GFP and GmMan1-RFP by dual wavelength microscopy in a Nipkov confocal laser scanning microscope. The results are presented in the form of a movie of 183-s duration (see Supplemental Videos 2 and 3 online), from which three frames (0, 61, and 183 s) are presented in Figures 10A to 10C. Three features are immediately apparent from these sequences. First, in agreement with data presented above, LeSec13:GFP fluorescent points greatly exceeded Golgi stacks (RFP-fluorescence) in number. Second, in confirmation of the observations of Nebenführ et al. (1999), not all Golgi stacks were simultaneously in movement. Thirdly, Golgi stacks were more often encountered with peripheral COPII fluorescence than not. Nevertheless, there are clear examples where a single Golgi stack moved into the plane of vision lacking associated LeSec13:GFP fluorescence but then was seen to be completely surrounded by them a few seconds later (cf. frames 34.4, 37.1, and 39.7 s in the third row of Figure 10B). We have also seen examples where a single Golgi stack, immobile for a period of many seconds, was present with and without COPII fluorescence (cf. frames 0.0 and 18.4 in Figure 10D). When the degree of LeSec13:GFP fluorescence surrounding an individual Golgi stack was plotted against the speed of movement of the stack (Figure 11), it became apparent that the slower a Golgi stack moves, the greater was the degree of COPII association. In surface view (i.e., looking at a stack from above or below) Golgi-associated COPII fluorescence appeared in the form of a partial or complete corona (see the third row of frames in Figure 10B, and Figure 10C). Rarely did we find images where the GFP and RFP signals were superimposed. Golgi stacks were also frequently seen in side view, where the RFP signal took the form of a cigar. Very often, however, the signal was only partially visible as red, and more often was yellow—the merge color. This observation indicates that COPII–Golgi interactions take place at the rim(s) of the Golgi cisternae rather than at their faces. These results also show that Golgi stacks do not have a fixed orientation with respect to the ER: as already reported by Nebenführ et al. (1999), they were observed to tumble as they move.

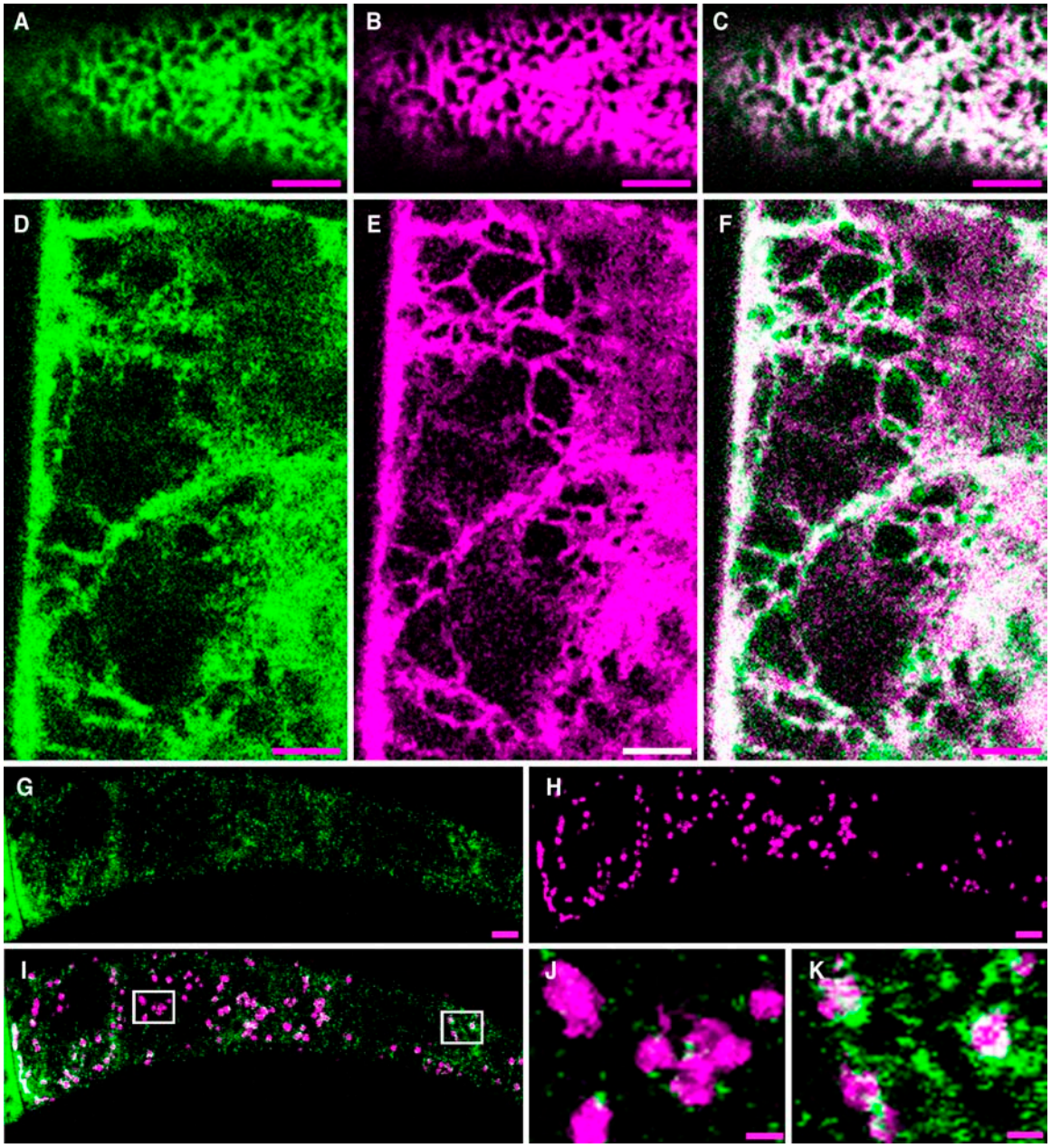

Figure 9. Labeling of ER and Golgi in BY-2 Cells Expressing LeSec13:GFP.

(A) and **(B)** Cortical ER in a cell coexpressing AtSec12-YFP **(A)** and AtBiP:DsRed **(B)**.
(C) Merge image for the cell depicted in **(A)** and **(B)**.
(D) An LeSec13:GFP expressing cell bombarded with AtBiP:DsRed; channel selected for green fluorescence.
(E) The same cell as in **(D)**, but channel selected for red fluorescence.
(F) Merge image for cell depicted in **(D)** and **(E)**.
(G) COPII labeling in a cell expressing LeSec13:GFP, which was bombarded with GmManI-RFP; channel selected for green fluorescence.
(H) The same cell as in **(G)**, but channel selected for red fluorescence.
(I) Merge image for cell depicted in **(G)** and **(H)**.
(J) and **(K)** High magnifications of two regions in **(I)** showing low and high density association of LeSec13:GFP with Golgi stacks.
Bars = 5 μm for all panels except **(J)** and **(K)** (1 μm).

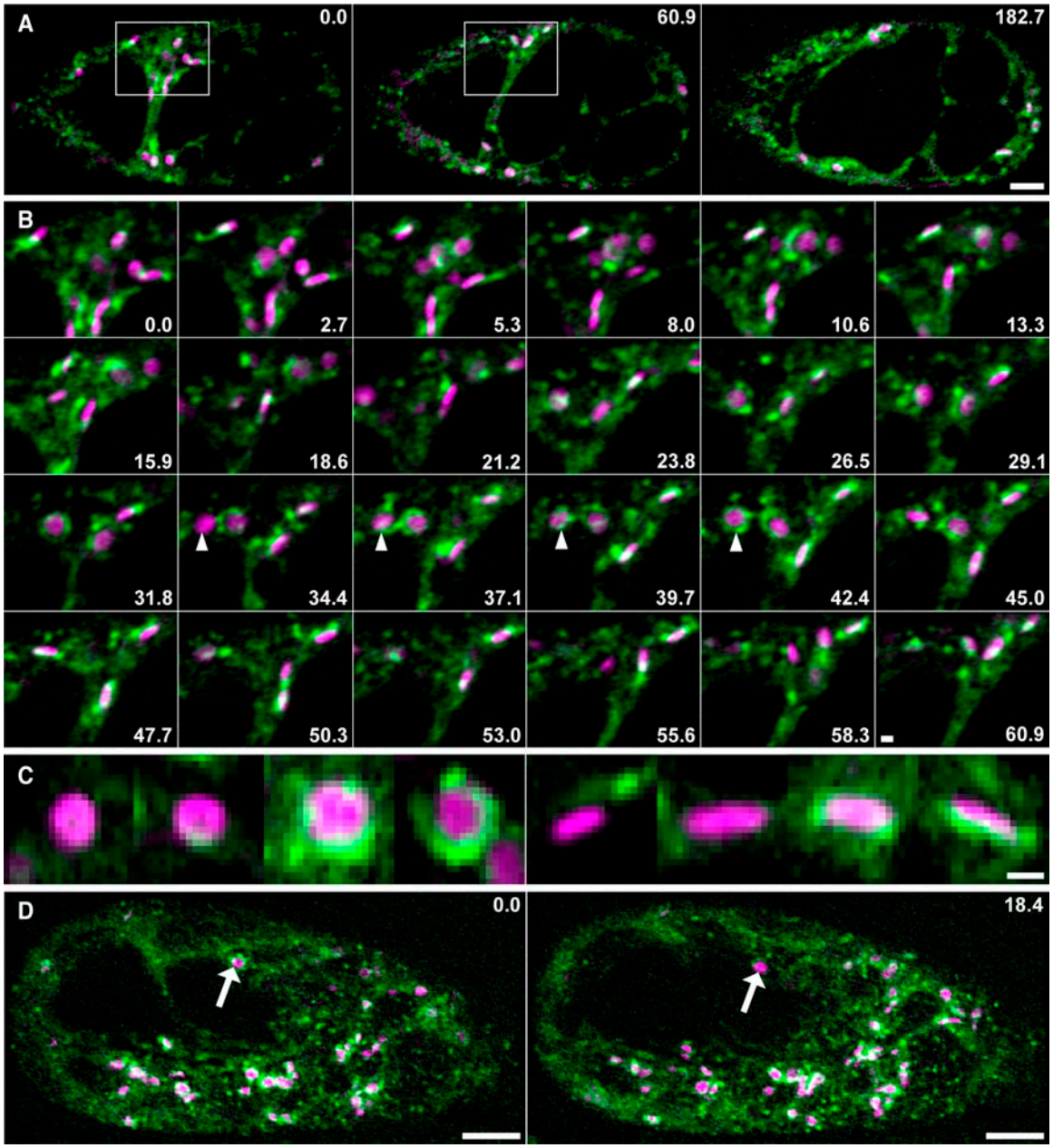

Figure 10. Analysis of LeSec13:GFP in Relation to the Golgi Apparatus by Time-Lapse Microscopy.

LeSec13:GFP-expressing cells were transformed by biolistics to coexpress GmManI:RFP and were monitored using an Ultra*VIEW* RS confocal microscope.

(A) and **(B)** Single optical sections images were acquired approximately every 2.6 s for 182.7 s (see Supplemental Video 2 online). LeSec13:GFP (green signal); GmManI:RFP (red signal).

(A) Images taken at 0, 60.9, and 182.7 s.

(B) Detailed views of the boxed area visible in Supplemental Video 2 online and in **(A)**. Numbers correspond to the time (in seconds). Arrowheads point to a single Golgi stack during four consecutive frames. Note that at 34.4 s very little LeSec13:GFP is associated with the Golgi stack, whereas at 42.4 s the same Golgi stack is completely surrounded by a halo of LeSec13:GFP.

(C) High-magnification pictures of Golgi stacks in face and side view (left and right panels, respectively), showing variable levels of association with LeSec13:GFP.

(D) Maximum intensity projection images of a cell coexpressing LeSec13:GFP and GmMan1:GFP viewed at a 18.4-s interval. Arrows point to the same Golgi stack that shows variable levels of association with LeSec13:GFP during time.

Bars = 5 μm in **(A)** and **(D)** and 1 μm in **(B)** and **(C)**.

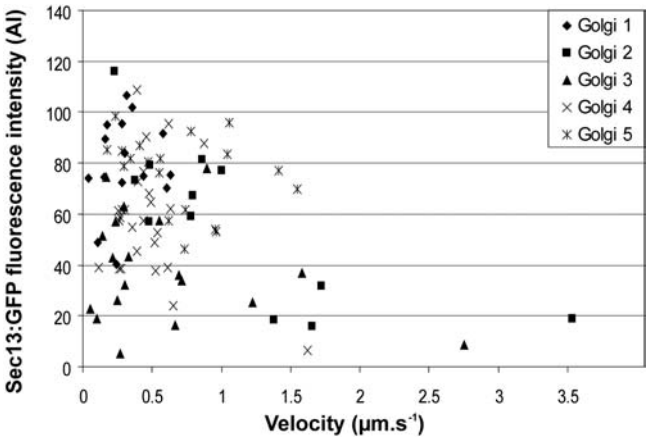

Figure 11. Analysis of Golgi COPII Association in Relation to Golgi Speed.

The net velocity of five individual Golgi stacks (from Supplemental Video 2 online) was measured at different times and plotted against the associated LeSec13:GFP fluorescence intensity in a fixed circular 5-μm^2 area around each Golgi stack.

DISCUSSION

COPII Visualization and Higher Plant ERES

The COPII coat on ERES in mammalian cells is known to develop sequentially: first by recruitment of Sar1-GTP to Sec12, then the sequestration of Sec23/24, followed by the binding of Sec13/31 (Barlowe, 2003; Bonifacino and Glick, 2004; Lee et al., 2004). Membrane-bound Sec13/31 should therefore represent fully assembled ERES and is the reason why the bulk of our observations have been made with Sec13 antibodies or with a transiently expressed LeSec13:GFP construct. Nevertheless, antibody staining with anti-Sar1 and anti-Sec23 gave rise to very similar patterns of COPII visualization. The validity of LeSec13:GFP as a marker for COPII is not only supported by its colocalization with Sec13 antibodies and by its localization to the nuclear envelope and nuclear matrix, which is the same for Sec13 in mammalian cells (Enninga et al., 2003), but also by its FRAP behavior. In addition, the expression of Sec13:GFP has no effect on the secretion index of protoplasts, whereas the expression of Sar1 mutants prevent export out of the ER and in the case of the Sar1-GDP mutant lead to an altered pattern of LeSec13:GFP fluorescence.

Although the interaction between Sec12 and Sar1-GTP is pivotal to the formation of ERES, Sec12 is excluded from COPII vesicles induced in vitro (Barlowe et al., 1994; Barlowe, 2002). In experiments when Sec12-GFP is expressed transiently, it would appear that the COPII GEF is distributed uniformly throughout the ER and not concentrated at ERES as might be expected. This has been described for *S. cerevisiae* (Rossanese et al., 1999), for mammalian cells (Weissman et al., 2001), and most recently for tobacco epidermal (daSilva et al., 2004) and BY-2 cells (this article). However, such fluorescent patterns are not in accordance with the discrete punctate visualization of COPII coat components as seen here and reported on numerous occasions elsewhere (Shugrue et al., 1999; Hammond and Glick, 2000; Stephens et al., 2000; Rust et al., 2001). An explanation for this discrepancy is not immediately apparent.

In contrast with Sec12, which is an integral membrane protein, Sar1 and the other COPII-coat proteins cycle on and off the ER membrane. As a consequence, these proteins can be detected at the surface of the ER (at ERES), in the cytosol as individual coat proteins, and theoretically on released COPII vesicles. Because of their lower local concentrations and higher diffusion rates, fluorescently labeled cytosolic COPII proteins give a weak, uniform, and diffuse signal, as seen in the nuclear matrix for Sec13 (Figures 4J and 5H to 5J). A similar diffuse cytosolic fluorescence can be observed for COPI components, especially after their release from Golgi membranes upon BFA treatment (Ritzenthaler et al., 2002a). This type of fluorescence is different to the punctate fluorescence seen for all COPII components. Those punctae not on or immediately adjacent to the ER may well represent released COPII vesicles, as suggested by Rust et al. (2001).

A consistent observation in our investigation, and one which contradicts the data presented by daSilva et al. (2004), is that COPII binding sites that we have visualized at the surface of the ER greatly outnumber that of the Golgi stacks. Although Golgi stacks temporarily associate with COPII principally at their rims, it is not clear whether the visualization of COPII binding is sufficient to allow these sites to be defined as ERES. This can only be done by showing in vivo that cargo molecules (membrane or lumenal) collect and exit from the ER at these sites. For the moment, we can therefore only regard the punctate COPII sites as being putative ERES. If each were an ERES, this would mean that COPII vesicles are formed and released with extreme rapidity because our live cell imaging data suggest that COPII cycles on and off the ER within seconds. However, the continual formation and release of COPII vesicles does not appear to be very plausible because it is difficult to understand how mobile Golgi stacks could efficiently collect this released cargo. An alternative scenario is that the punctate COPII sites are potential ERES, but the completion of vesicle budding and release is only triggered upon arrival and docking of a Golgi stack. As a consequence, this would mean that a large portion of the COPII-coat proteins are involved in futile cycles of binding and dissociation. At the least, this would indicate that Sec13, and the other COPII-coat proteins for that matter, are not a limiting factor in the ER-to-Golgi transport in plants. Indeed, their overexpression, as demonstrated here and by daSilva et al. (2004), is without effect on secretion.

Randomly distributed ERES in mammalian cells are relatively immobile (displacement time of 5 to 15 $\mu m \cdot h^{-1}$; Stephens, 2003) in comparison with the rate of cargo transport between the cortical ER and the perinuclear Golgi apparatus (0.5 to 1 $\mu m \cdot s^{-1}$; Stephens et al., 2000). As previously mentioned, ERGIC/VTCs are responsible for this long-range transport, and these are generally considered to arise from the homotypic fusion of COPII vesicles (Stephens and Pepperkok, 2001; Duden, 2003). It would appear that each ERGIC/VTC is formed from a single ERES (Stephens et al., 2000). Upon completion of mitosis in mammalian cells, ERES form de novo (frequency: 2 $h^{-1} \cdot 100\ \mu m^{-2}$) and

continue to do so during interphase and remain visible for several minutes (Stephens, 2003). During this time, COPII proteins continually cycle on and off the membrane but with different kinetics for each of the three major components (Sar1, Sec23/24, and Sec13/31; R. Forster, D. Stephens, and R. Pepperkok, unpublished data). According to Stephens (2003), ERES can also fuse with one another and divide. In common with mammalian cells, ERES in BY-2 cells are quite stationary, but they appear to be more dynamic structures than their mammalian counterparts: individual ERES were rarely visible for periods longer than a few seconds. Because of this property, it was not possible to ascertain whether plant ERES aggregate and/or divide. It could also be the reason why the visualization of COPII budding in plants by electron microscopy has been so elusive.

It is well known that during mitosis the Golgi apparatus in mammalian cells breaks down into vesicles (Shorter and Warren, 2002). It has been claimed that these vesicles, together with Golgi matrix proteins that are required as a scaffold for the reconstitution of the Golgi apparatus at the onset of the subsequent interphase, lie in close proximity to ERES whose function is arrested during mitosis (Prescott et al., 2001; Seemann et al., 2002). Immunostaining with COPII antisera has suggested that ERES were nonetheless still visible during mitosis (Prescott et al., 2001). However, the recently published data of Stephens (2003) indicates that this visualization is artifactual in nature: live cell imaging with YFP-Sec23 clearly showed a displacement of COPII into the cytosol during mitosis. In plants, the Golgi apparatus does not fragment during mitosis, and in BY-2 cells, many Golgi stacks appear to be immobilized in the immediate vicinity of the mitotic spindle (Nebenführ et al., 2000). However, during telophase, the plant Golgi apparatus is particularly active in secreting to the forming cell plate. As shown by Segui-Simarro et al. (2004), Golgi stacks enter the phragmoplast between the daughter nuclei during late telophase, where increasing amounts of ER are also to be found. Such a stage is comparable to that depicted in Figures 3F and 3G. Consistent with this are our results, obtained by live cell imaging with LeSec13:GFP, which demonstrate that ERES are visible within the phragmoplast and are presumably functionally intact.

BFA and ERES

BFA has been a most useful tool in investigations into the secretory and endocytic pathways (reviewed in Nebenführ et al., 2002). Research on mammalian and fungal cells has established that this drug interacts with a complex formed between the GTPase ADP ribosylation factor (ARF) and its GEF (Peyroche et al., 1999). The discovery that the Arabidopsis protein GNOM, which is important for the correct targeting of the auxin efflux carrier PIN1 to the plasma membrane, is a BFA-sensitive ARF-GEF (Geldner et al., 2003, 2004) now makes it very likely that the molecular target for BFA is the same for all eukaryotic cells.

ARF-GEFs have so far not been reported at the ER in any cell type, so claims that BFA can act at the level of ERES (Brandizzi et al., 2002; daSilva et al., 2004; Hawes and Brandizzi, 2004) require experimental substantiation. Our results showing that BFA has little effect on the ability to recognize COPII binding sites are in agreement with anti-Sec31 staining data obtained on NRK cells (Puri and Linstedt, 2003). However, as such these results say nothing about the export competence of the ERES so visualized. Ward et al. (2001) previously showed that COPII components still cycle at ERES after addition of BFA. More recent FRET measurements performed on Vero cells indicate that BFA interferes with the kinetics of the interaction between Sec23 and Sec31, whereas the interaction between Sar1 and Sec23 remained unaltered (R. Forster, D. Stephens, and R. Pepperkok, unpublished data). However, treatment with BFA for short periods, during which time COPI assembly was inhibited, did not alter the steady state distribution of any COPII component. Thus, it seems likely that any effect of BFA on ER export is an indirect one resulting from a perturbation in the fine tuning of the interdependent COPI and COPII machineries (Stephens et al., 2000; Ward et al., 2001), upon whose maintenance successful ER–Golgi transport depends.

ERES and the Golgi Apparatus: Models and Data

Currently, there are three models that have been put forward to explain ER-to-Golgi transport in plants (Neumann et al., 2003). In the earliest of these, Golgi stacks were considered to sweep up export vesicles as they moved over the surface of the ER (the vacuum cleaner model; Boevink et al., 1998). By contrast, the stop-and-go model of Nebenführ et al. (1999) foresees cargo collection restricted only to those Golgi stacks that have temporarily come to a halt over an ERES. According to the third, mobile secretory unit concept (Neumann et al., 2003), each individual Golgi stack has its own ERES and both travel together across the surface of the ER. This means that ERES and Golgi stacks must be identical in number and intracellular distribution, that both are motile, and, finally, that ERES should be long-lived entities.

Support for this latter model has recently been presented by daSilva et al. (2004), who have investigated the distribution of AtSar1-YFP, AtERD2-GFP, and the Golgi marker ST-GFP by transient expression in tobacco epidermis. According to these authors, these two constructs were constantly located together into ''distinct but overlapping structures,'' and that this tandem structure was mobile in an actin-dependent manner. A degree of permanency for this structure was suggested by selective photobleaching of the YFP signal that inevitably recovered in the immediate vicinity of the GFP signal. In complete contradiction with the secretory unit concept, our results show that several ERES can attach to a single Golgi stack at any one time and that ERES are not constantly associated with the Golgi apparatus, assuming of course that each punctate COPII labeling represents one ERES (see above). Moreover, Golgi-ERES associations are not permanent but are continually changing in number and position at the rims of the stack as the Golgi moves. Another important distinction between our data and that of daSilva et al. (2004) relates to the relative apparent sizes of the Golgi and ERES images. In the latter article, these two structures appear to be of similar size, but in our work, ERES appear significantly smaller. Thus, our observations are more in keeping with a kiss-and-run model for ER-to-Golgi transport.

A feature common to the vacuum cleaner and stop-and-go models is that ERES outnumber Golgi stacks and are relatively stationary. This is supported by the data presented here. However, in the sense that ERES are seen at the rims of both stationary and moving Golgi stacks in BY-2 cells, our data do not exactly conform with the latter model. Indeed, we have demonstrated that a stationary Golgi stack can be visualized over a 20-s period both with and without associated peripheral ERES. Thus, Golgi motility per se does not seem to be a precondition for successful ER-to-Golgi transport, and this is in agreement with FRAP measurements dealing with the recovery of photobleached Golgi marker proteins on immobilized (Brandizzi et al., 2002) and moving (Brandizzi and Hawes, 2004) Golgi stacks.

Mobility is a crucial feature of the mobile secretory unit model, even though it remains unclear as to how a Golgi stack and its associated ERES remain together during movement. However, this is important because if true it would mean that a Golgi stack would have to drag its ERES through a lipid membrane. In our opinion, this can only be achieved through direct physical continuities (tubular ER-Golgi connections) or through the existence of some kind of scaffolding elements linking the two together. The former possibility has previously been suggested (Brandizzi and Hawes, 2004; Hawes and Brandizzi, 2004), but always in neglect of retrograde COPI vesicle transport, which does seem to exist in plants (Pimpl et al., 2000; Ritzenthaler et al., 2002a). Evidence for the latter is lacking. With regard to Golgi motility we would like, in addition, to point out some inconsistencies in the data published using the tobacco leaf epidermis and BY-2 cell systems. According to Boevink et al. (1998), Golgi stacks in epidermal cells move with speeds of up to 0.76 $\mu m \cdot s^{-1}$ along stationary cortical ER and in excess of 2.2 $\mu m \cdot s^{-1}$ within transvacuolar cytoplasmic strands. In the article by daSilva et al. (2004), the speed of Golgi stacks lies between 0.1 and 0.3 $\mu m \cdot s^{-1}$ (calculated from the values given in Figure 9 of that article). These latter values contrast with those determined for Golgi stacks in BY-2 cells ($\sim$3 $\mu m \cdot s^{-1}$) by Nebenführ et al. (1999) and confirmed here. In fact, such low velocities are in the range of the almost stationary wiggling motion described by Nebenführ et al. (1999) for BY-2 cells. Because our data suggest that the degree of Golgi-COPII association increases the slower the Golgi moves, which is understandable, we would therefore plead for more caution in the interpretation of the temporal aspect of ERES-Golgi associations.

The differences in the depiction of the ERES and Golgi stacks as given in our article and that of daSilva et al. (2004) may well lie in the relative secretory status of the cell types employed in the two studies. Tobacco BY-2 cells represent a rapidly growing and dividing cell system with a high rate of secretion. Tobacco leaf epidermal cells, on the other hand, hardly grow, do not divide, and will obviously be secreting at a much lower level. Thus, one might consider the leaf epidermis to represent a kind of minimal system, with membrane trafficking to the cell surface and within the endomembrane system being reduced to a housekeeping role. In this situation, ER export will not be comparable to that in BY-2 cells: the number of ERES may well be reduced to a level where their number approximates that of the Golgi stacks. This being the case, it is probably more efficient to have a Golgi stack hovering in the vicinity of a more or less stationary ERES than to be rapidly wandering across the surface of an ER with few exit sites. By contrast, a situation where ERES greatly outnumber Golgi stacks would have advantages for a rapidly secreting system, such as BY-2 cells, because it would allow more material to be sorted at the ER and secreted per unit of time. It also would be more robust toward distortions because missing a few events would not matter, whereas the secretory unit model would require much more stringent regulatory mechanisms.

METHODS

Materials

Suspension cultures of Bright Yellow 2 (BY-2) tobacco (*Nicotiana tabacum*) were maintained at 27°C in MS medium (Sigma-Aldrich, Taufkirchen, Germany). *Arabidopsis thaliana* var *Columbia* cell suspensions were cultured in Gamborg's B5 Medium (Sigma-Aldrich G5893). Cells were maintained in the log phase by subculturing weekly into fresh medium at a dilution of 1:50. In addition to wild-type cells, two stably transformed BY-2 cell lines were also employed: one expressing the Golgi marker α-mannosidase 1-GFP from *Glycine max* (GmMan1:GFP; Nebenführ et al., 1999); the other expressing the ER-localized fusion construct GFP:HDEL (Nebenführ et al., 2000). For secretory index determinations (see below), tobacco plants (*N. tabacum* cv Petite Havana) were grown on agar under sterile conditions as given in Crofts et al. (1999) and daSilva et al. (2004).

Generation of Recombinant Proteins and Preparation of Antisera

The preparation of recombinant AtSec13 and AtSec23 and the generation of affinity-purified antibodies (from rats, AtSec13; from rabbits, AtSec23) have previously been given (Movafeghi et al., 1999; Contreras et al., 2004). AtSec12b (accession number BAB09140, Arabidopsis Biological Resource Center, The Ohio State University, Columbus, OH) was amplified from the CD4-7 cDNA library. The cytosolic domain was cloned into the *Eco*RI and *Sma*I sites in pGEX4T3 (Amersham Biosciences Europe, Freiburg, Germany). A GST fusion protein was produced and purified from *Escherichia coli* as previously described (Movafeghi et al., 1999). Polyclonal antibodies in rats were generated commercially (Biosciences, Göttingen, Germany) and affinity purified using a GST-AtSec12b-Sepharose 4B column.

Stable Transformation of BY-2 Cells with LeSec13:GFP

A tomato (*Lycopersicon esculentum*) EST clone (accession number AI776423) closely homologous to AtSec13 was ordered from Clemson University Genomics Institute (Clemson, SC). A full length of LeSec13 was amplified by PCR and cloned into pCK(X/S) LTEV-EGFP (Ritzenthaler et al., 2002b) to obtain pCK-LeSec13-EGFP. The LeSec13-EGFP was then subcloned into the pTA7002 vector (Aoyama and Chua, 1997) for creating an inducible LeSec13-EGFP stable transformant. PTA7002-LeSec13-EGFP was introduced into the LBA4404 strain of *Agrobacterium tumefaciens* by the freeze-thaw method (An et al., 1988).

Transformation of BY-2 cells was done by coculturing a 3-d-old BY-2 culture with a 36-h-old LBA4404 culture. The coculture was incubated in the dark without shaking for 2 d at 25°C. The cells were pelleted and washed three times in fresh medium containing 250 μg/mL of carbenicilin. After a final wash, the suspension was poured on the solid medium containing carbenicilin and hygromycin. Positive calli (obtained after several weeks) were screened by fluorescence microscopy to select the best cell lines. Expression of LeSec13:GFP in the BY-2 cells was initiated

by the addition of 10 μM dexamethasone (Sigma-Aldrich). After 24 to 30 h of incubation, samples were removed for microscopy.

Preparation of a Cytosol and Total Membrane Fractions

Arabidopsis cells were harvested and resuspended in prechilled buffer [25 mM Hepes/KOH, pH 8.0, 300 mM sucrose, 10 mM KCl, 3 mM EDTA, 1 mM DTT, 2 mM *o*-phenanthroline, 1.4 mg/L pepstatin, 0.5 mg/L leupeptin, 2 mg/L aprotinin, and 1 mg/mL 2,1 *trans*-epoxysuccinyl-L-leucylamido-(4-guanido)-butane] using a Waring blender with three 15-s bursts. The slurry was then passed through two layers of Miracloth (Calbiochem, San Diego, CA) and four layers of gauze. After precentrifugation at 5000*g* for 20 min, total membranes were pelleted at 100,000*g* for 1 h. The concentration of protein was determined by dye binding (Bradford, 1976). BY-2 cytosol and membranes were prepared as above, except that the cells were broken in a Jeda press (Linca-Lamon Instrumentation, Rehovot, Israel).

Sucrose Gradient Analysis

The supernatant of a 5000-g Arabidopsis cell homogenate (prepared as above, but in the presence of 0.1 mM EDTA and 3 mM $MgCl_2$) was centrifuged onto a 60% (w/w) sucrose cushion. The interface was carefully removed and loaded onto a linear 20 to 55% (w/w) sucrose gradient. After centrifugation at 100,000*g* in a swing-out rotor for 16 h, 1.5-mL fractions were collected.

Gel Electrophoresis and Protein Gel Blotting

Protein in microsomal, cytosol, and sucrose gradient fractions were precipitated out using the chloroform/methanol procedure of Wessel and Flügge (1984) and separated by 10% SDS-PAGE. Protein gel blotting and marker antibodies (reversibly glycosylated polypeptide; calnexin) were as previously given (Pimpl et al., 2000). Primary dilutions for the COPII antisera were as follows: 1:500 (anti-AtSec12b, anti-AtSec13, and anti-AtSec23) and 1:2000 (anti-AtSar1).

Preparation of RFP Constructs and Biolistic Transformation

The monomeric RFP (Campbell et al., 2002) was amplified using DSR2-30For and DSR2-30Re as primers and cloned into pGreen0029 Sp::GFP-HDEL (Hellens et al., 2000) to replace GFP. The *Bam*HI-*Sac*I fragment was excised from this vector and subcloned into a p35S vector to create p35S-Sp:RFP for transient expression. For GmManI-RFP, the same procedure was employed except that the PCR-amplified RFP was subcloned into the BP30 vector of Nebenführ et al. (1999) to get pBP30-GmManI:RFP. The LeSec13:GFP-expressing cell line was transfected by biolistics using the procedure described by Vetter et al. (2004). Cells were observed between 18 and 24 h post-transfection except for BiP:DsRed, which was visualized between 36 and 48 h post-transfection. The dominant-negative NtSar1 GDP-fixed mutant was obtained from Masaki Takeuchi (RIKEN Institute, Waco, Japan).

Secretory Index Determinations

Protoplasts were isolated from tobacco leaves exactly as described by Crofts et al. (1999) and subjected to electroporation with DNA encoding for the secretory enzyme α-amylase together with DNA encoding for the effector protein under consideration as given by Phillipson et al. (2001) and daSilva et al. (2004). Plasmid concentrations are given in Figure 3. After incubation for 24 h, the protoplasts were separated from the extracellular medium. Preparation of fractions and determination of extracellular (secreted) and intracellular α-amylase activities were performed exactly as given by Crofts et al. (1999). The secretory index is defined as the ratio of extracellular to intracellular activities, whereby the total activity represents the sum of the α-amylase activities in the medium and the protoplasts (Denecke et al., 1990). The presence of expressed effector proteins in the homogenates of the protoplasts was determined as described by daSilva et al. (2004) using antibodies against GFP (Molecular Probes, Eugene, OR) and AtSar1 (see above) for the detection of Sec13-GFP and Sar1[H74L], respectively.

Confocal Laser Scanning Microscopy

Before observation, fixed cells were mounted in a chamber containing PBS and 0.1% Na ascorbate, pH 7.4, to reduce photobleaching. The living cells were allowed to settle onto a poly-L-Lys–coated cover slip that was mounted in a chamber containing 400 μL of fresh BY-2 medium. Cells were observed with a Zeiss LSM510 laser scanning confocal microscope (Jena, Germany) using a C-APOCHROMAT (63× 1.2 W Korr) water objective lens in multitrack mode. Excitation/emission wavelengths were 488 nm/505 to 545 nm for GFP and 543/long-pass 560 nm for Alexa-fluor 568, DsRed, and mRFP. Transmitted light reference images were captured using differential interference contrast optics and argon laser illumination at 488 nm. The images are presented as single sections or stacks of neighboring sections as stated in the figure legends. LSM 510 three-dimensional reconstruction functions were employed to compute projections of serial confocal sections. Image processing was performed with LSM510 version 2.8 (Zeiss), ImageJ (National Institutes of Health, http://rsb.info.nih.gov/ij/), and Photoshop 6.0 (final image assembly; Adobe Systems, San Jose, CA).

Immunofluorescence Labeling

The procedures were performed as described previously (Ritzenthaler et al., 2002a; Laporte et al., 2003). Primary antibody dilutions were as follows: 1:1000 (anti-AtSec23 and anti-AtSar1) and 1:100 (anti-AtSec13). Secondary antibodies (Alexa-fluor 568 goat anti-rabbit or anti-mouse IgG) were used at 1:300 dilution.

FRAP

Experiments were performed on a Zeiss LSM510 confocal microscope in a similar manner to that described by Enninga et al. (2003). BY-2 cells expressing LeSec13:GFP or EGFP alone were selected for the experiments and monitored with a 488-nm argon laser line at 70% laser power and 5% transmission (imaging intensity). For FRAP analyses, three imaging scans of the area of interest were performed, and then a specific region was selected for bleaching. Twenty bleaching iterations were performed with 75% laser power and 100% transmittance. Then, scans were taken every 30 s during the course of fluorescence recovery until the fluorescence intensity reached a plateau. FRAP recovery curves were generated from background subtracted images, and fluorescence was normalized by measuring the fluorescence intensity of an unbleached adjacent cell. The normalized fluorescence was determined for each image and compared with the initial normalized fluorescence to determine the amount of signal lost during the bleach pulse and during imaging. The equation used for these calculations has been described previously (Phair and Misteli, 2000).

Live Cell Imaging

BY-2 cells expressing LeSec13:GFP only or together with GmManI:RFP were first allowed to settle onto a poly-L-Lys–coated cover slip mounted in a chamber containing 400 μL of fresh BY-2 medium. Imaging was performed with a Perkin-Elmer Ultra*VIEW* RS spinning disk confocal microscope (Foster City, CA), fitted with an argon 488-nm laser and a

543-nm HeNe ion laser, and using a ×100 1.45–numerical aperture oil immersion lens (Nikon, Tokyo, Japan). Cells were observed (single optical sections or z sections of 0.2 μm) for up to 5 min under continuous irradiation without noticeable photobleaching. The number and diameter of the LeSec13:GFP fluorescent structures as well as the size and speed of Golgi stacks were measured using ImageJ. Thresholding was applied to the images to reduce background noise.

Image Processing

Image processing was conducted with LSM510 version 2.8, ImageJ, and Photoshop 6.0 (final image assembly). Golgi velocity was measured as previously described (Nebenführ et al., 1999).

Sequence data from this article have been deposited with the EMBL/GenBank data libraries under accession numbers A1776423 and BAB09140.

ACKNOWLEDGMENTS

We gratefully acknowledge the financial support of the Deutsche Forschungsgemeinschaft. We thank Masaki Takeuchi and Jürgen Denecke for providing us with the GDP- and GTP-fixed Sar1 mutants. We also thank Inhwan Hwang for giving us the BiP clone and Chris Hawes for the Sec12-YFP construct. The technical assistance of Sara Duval is gratefully acknowledged. We also appreciate having had useful discussions at various stages during this investigation with Jürgen Denecke, Andreas Nebenführ, and Christiane Stussi-Garaud. The Inter-Institute Zeiss LSM510 confocal microscopy platform was cofinanced by the Centre National de la Recherche Scientifique, the Université Louis Pasteur, the Région Alsace, the Association de la Recherche sur le Cancer, and the Ligue Nationale contre le Cancer.

Received August 10, 2004; accepted March 3, 2005.

REFERENCES

An, G., Ebert, P.R., Mitra, A., and Ho, S. B . (1988). Binary vectors. In Plant Molecular Biology Manual, S.B. Gelvin and R.A. Schilperoort, eds (Dordrecht, The Netherlands: Kluwer Academic Publishers), pp. 3–7.

Andreeva, A.V., Kutuzov, M.A., Evans, D.E., and Hawes, C.R. (1998). Proteins involved in membrane transport between the ER and the Golgi apparatus: 21 putative plant homologues revealed by dbEST searching. Cell Biol. Int. **22,** 145–160.

Antonny, B., and Schekman, R. (2001). ER export: Public transportation by the COPII coach. Curr. Opin. Cell Biol. **13,** 438–443.

Aoyama, T., and Chua, N. (1997). A glucocorticoid-mediated transcriptional induction system in transgenic plants. Plant J. **11,** 605–612.

Aridor, M., and Balch, W.E. (2000). Kinase signaling initiates coat complex II (COPII) recruitment and export from the mammalian endoplasmic reticulum. J. Biol. Chem. **275,** 35673–35676.

Aridor, M., Fish, K.N., Bannykh, S., Weissman, J., Roberts, T.H., Lippincott-Schwartz, J., and Balch, W.E. (2001). The Sar1 GTPase coordinates biosynthetic cargo selection with endoplasmic reticulum export site assembly. J. Cell Biol. **152,** 213–229.

Bannykh, S.I., Rowe, T., and Balch, W.E. (1996). The organization of endoplasmic reticulum export complexes. J. Cell Biol. **135,** 19–35.

Barlowe, C. (1998). COPII and selective export from the endoplasmic reticulum. Biochim. Biophys. Acta **1404,** 67–76.

Barlowe, C. (2002). COPII-dependent transport from the endoplasmic reticulum. Curr. Opin. Cell Biol. **14,** 417–422.

Barlowe, C. (2003). Signals for COPII-dependent export from the ER: What's the ticket out? Trends Cell Biol. **13,** 295–300.

Barlowe, C., Orci, L., Yeung, T., Hosobuchi, M., Hamamoto, S., Salama, N., Rexach, M.F., Ravazzola, M., Amherdt, M., and Schekman, R. (1994). COPII: A membrane coat formed by Sec proteins that drive vesicle budding from the endoplasmic reticulum. Cell **77,** 895–907.

Barlowe, C., and Schekman, R. (1993). SEC12 encodes a guanine-nucleotide-exchange factor essential for transport vesicle budding from the ER. Nature **365,** 347–349.

Bar-Peled, M., and Raikhel, N.V. (1997). Characterization of AtSEC12 and AtSAR1. Proteins likely involved in endoplasmic reticulum and Golgi transport. Plant Physiol. **114,** 315–324.

Bevis, B.J., Hammond, A.T., Reinke, C.A., and Glick, B.S. (2002). De novo formation of transitional ER sites and Golgi structures in *Pichia pastoris*. Nat. Cell Biol. **4,** 750–756.

Bi, X., Corpina, R.A., and Goldberg, J. (2002). Structure of the Sec23/24-Sar1 pre-budding complex of the COPII vesicle coat. Nature **419,** 271–277.

Boevink, P., Oparka, K., Santa Cruz, S., Martin, B., Betteridge, A., and Hawes, C. (1998). Stacks on tracks: The plant Golgi apparatus traffics on an actin/ER network. Plant J. **15,** 441–447.

Bonifacino, J.S., and Glick, B.S. (2004). The mechanisms of vesicle budding and fusion. Cell **116,** 153–166.

Bradford, M.M. (1976). A rapid and sensitive method for the quantitation of microgram quantities of protein utilizing the principle of protein-dye binding. Anal. Biochem. **72,** 248–254.

Brandizzi, F., and Hawes, C. (2004). A long and winding road: Symposium on membrane trafficking in plants. EMBO Rep. **5,** 245–249.

Brandizzi, F., Snapp, E.L., Roberts, A.G., Lippincott-Schwartz, J., and Hawes, C. (2002). Membrane protein transport between the endoplasmic reticulum and the Golgi in tobacco leaves is energy dependent but cytoskeleton independent: Evidence from selective photobleaching. Plant Cell **14,** 1293–1309.

Campbell, R.E., Tour, O., Palmer, A.E., Steinbach, P.A., Baird, G.S., Zacharias, D.A., and Tsien, R.Y. (2002). A monomeric red fluorescent protein. Proc. Natl. Acad. Sci. USA **99,** 7877–7882.

Contreras, I., Ortiz-Zapater, E., and Aniento, F. (2004). Sorting signals in the cytosolic tail of membrane proteins involved in the interaction with plant ARF1 and coatomer. Plant J. **38,** 685–698.

Contreras, I., Ortiz-Zapater, E., Castilho, L.M., and Aniento, F. (2000). Characterization of Cop I coat proteins in plant cells. Biochem. Biophys. Res. Commun. **273,** 176–182.

Craig, S., and Staehelin, L.A. (1988). High pressure freezing of intact plant tissues. Evaluation and characterization of novel features of the endoplasmic reticulum and associated membrane systems. Eur. J. Cell Biol. **46,** 81–93.

Crofts, A.J., Leborgne-Castel, N., Hillmer, S., Robinson, D.G., Phillipson, B., Carlsson, L.E., Ashford, D.A., and Denecke, J. (1999). Saturation of the endoplasmic reticulum retention machinery reveals anterograde bulk flow. Plant Cell **11,** 2233–2248.

daSilva, L.L., Snapp, E.L., Denecke, J., Lippincott-Schwartz, J., Hawes, C., and Brandizzi, F. (2004). Endoplasmic reticulum export sites and Golgi bodies behave as single mobile secretory units in plant cells. Plant Cell **16,** 1753–1771.

Denecke, J., Botterman, J., and Deblaere, R. (1990). Protein secretion in plant cells can occur via a default pathway. Plant Cell **2,** 51–59.

Duden, R. (2003). ER-to-Golgi transport: COP I and COP II function (Review). Mol. Membr. Biol. **20,** 197–207.

Enninga, J., Levay, A., and Fontoura, B.M. (2003). Sec13 shuttles

between the nucleus and the cytoplasm and stably interacts with Nup96 at the nuclear pore complex. Mol. Cell. Biol. **23,** 7271–7284.

Geldner, N., Anders, N., Wolters, H., Keicher, J., Kornberger, W., Muller, P., Delbarre, A., Ueda, T., Nakano, A., and Jurgens, G. (2003). The Arabidopsis GNOM ARF-GEF mediates endosomal recycling, auxin transport, and auxin-dependent plant growth. Cell **112,** 219–230.

Geldner, N., Richter, S., Vieten, A., Marquardt, S., Torres-Ruiz, R.A., Mayer, U., and Jurgens, G. (2004). Partial loss-of-function alleles reveal a role for GNOM in auxin transport-related, post-embryonic development of Arabidopsis. Development **131,** 389–400.

Hammond, A.T., and Glick, B.S. (2000). Dynamics of transitional endoplasmic reticulum sites in vertebrate cells. Mol. Biol. Cell **11,** 3013–3030.

Hawes, C., and Brandizzi, F. (2004). The Golgi apparatus—Still causing problems after all these years! Cell. Mol. Life Sci. **61,** 131–132.

Hellens, R.P., Edwards, E.A., Leyland, N.R., Bean, S., and Mollineaux, P.M. (2000). pGreen: A versatile and flexible binary Ti vector for Agrobacterium-mediated plant transformation. Plant Mol. Biol. **42,** 819–832.

Horstmann, H., Ng, C.P., Tang, B.L., and Hong, W. (2002). Ultrastructural characterization of endoplasmic reticulum–Golgi transport containers (EGTC). J. Cell Sci. **115,** 4263–4273.

Jürgens, G. (2004). Membrane trafficking in plants. Annu. Rev. Cell Dev. Biol. **20,** 481–504.

Klumperman, J. (2000). Transport between ER and Golgi. Curr. Opin. Cell Biol. **12,** 445–449.

Ladinsky, M.S., Mastronarde, D.N., McIntosh, J.R., Howell, K.E., and Staehelin, L.A. (1999). Golgi structure in three dimensions: Functional insights from the normal rat kidney cell. J. Cell Biol. **144,** 1135–1149.

Laporte, C., Vetter, G., Loudes, A.M., Robinson, D.G., Hillmer, S., Stussi-Garaud, C., and Ritzenthaler, C. (2003). Involvement of the secretory pathway and the cytoskeleton in intracellular targeting and tubule assembly of *Grapevine fanleaf virus* movement protein in tobacco BY-2 cells. Plant Cell **15,** 2058–2075.

Lee, M.C.S., Miller, E.A., Goldberg, J., Orci, L., and Schekman, R. (2004). Bi-directional protein transport between the ER and Golgi. Annu. Rev. Cell Dev. Biol. **20,** 87–123.

Miller, E., Antonny, B., Hamamoto, S., and Schekman, R. (2002). Cargo selection into COPII vesicles is driven by the Sec24p subunit. EMBO J. **21,** 6105–6113.

Mogelsvang, S., Gomez-Ospina, N., Soderholm, J., Glick, B.S., and Staehelin, L.A. (2003). Tomographic evidence for continuous turnover of Golgi cisternae in *Pichia pastoris*. Mol. Biol. Cell **14,** 2277–2291.

Mossessova, E., Bickford, L.C., and Goldberg, J. (2003). SNARE selectivity of the COPII coat. Cell **114,** 483–495.

Movafeghi, A., Happel, N., Pimpl, P., Tai, G.H., and Robinson, D.G. (1999). Arabidopsis Sec21p and Sec23p homologs. Probable coat proteins of plant COP-coated vesicles. Plant Physiol. **119,** 1437–1446.

Murshid, A., and Presley, J.F. (2004). ER-to-Golgi transport and cytoskeletal interactions in animal cells. Cell. Mol. Life Sci. **61,** 133–145.

Nebenführ, A., Frohlick, J.A., and Staehelin, L.A. (2000). Redistribution of Golgi stacks and other organelles during mitosis and cytokinesis in plant cells. Plant Physiol. **124,** 135–151.

Nebenführ, A., Gallagher, L.A., Dunahay, T.G., Frohlick, J.A., Mazurkiewicz, A.M., Meehl, J.B., and Staehelin, L.A. (1999). Stop-and-go movements of plant Golgi stacks are mediated by the acto-myosin system. Plant Physiol. **121,** 1127–1142.

Nebenführ, A., Ritzenthaler, C., and Robinson, D.G. (2002). Brefeldin A: Deciphering an enigmatic inhibitor of secretion. Plant Physiol. **130,** 1102–1108.

Neumann, U., Brandizzi, F., and Hawes, C. (2003). Protein transport in plant cells: In and out of the Golgi. Ann. Bot. (Lond.) **92,** 167–180.

Orci, L., Ravazzola, M., Meda, P., Holcomb, C., Moore, H.P., Hicke, L., and Schekman, R. (1991). Mammalian Sec23p homologue is restricted to the endoplasmic reticulum transitional cytoplasm. Proc. Natl. Acad. Sci. USA **88,** 8611–8615.

Otte, S., and Barlowe, C. (2002). The Erv41p-Erv46p complex: Multiple export signals are required in trans for COPII-dependent transport from the ER. EMBO J. **21,** 6095–6104.

Otte, S., Belden, W.J., Heidtman, M., Liu, J., Jensen, O.N., and Barlowe, C. (2001). Erv41p and Erv46p: New components of COPII vesicles involved in transport between the ER and Golgi complex. J. Cell Biol. **152,** 503–518.

Palade, G. (1975). Intracellular aspects of the process of protein synthesis. Science **189,** 347–358.

Pavelka, M., and Robinson, D.G. (2003). The Golgi apparatus in mammalian and higher plant cells: A comparison. In The Golgi Apparatus and the Plant Secretory Pathway, D.G. Robinson, ed (Oxford: Blackwell Publishing), pp. 16–35.

Peyroche, A., Antonny, B., Robineau, S., Acker, J., Cherfils, J., and Jackson, C.L. (1999). Brefeldin A acts to stabilize an abortive ARF-GDP-Sec7 domain protein complex: Involvement of specific residues of the Sec7 domain. Mol. Cell **3,** 275–285.

Phair, R.D., and Misteli, T. (2000). High mobility of proteins in the mammalian cell nucleus. Nature **404,** 604–609.

Phillipson, B.A., Pimpl, P., daSilva, L.L., Crofts, A.J., Taylor, J.P., Movafeghi, A., Robinson, D.G., and Denecke, J. (2001). Secretory bulk flow of soluble proteins is efficient and COPII dependent. Plant Cell **13,** 2005–2020.

Pimpl, P., Movafeghi, A., Coughlan, S., Denecke, J., Hillmer, S., and Robinson, D.G. (2000). In situ localization and in vitro induction of plant COPI-coated vesicles. Plant Cell **12,** 2219–2236.

Prescott, A.R., Farmaki, T., Thomson, C., James, J., Paccaud, J.P., Tang, B.L., Hong, W., Quinn, M., Ponnambalam, S., and Lucocq, J. (2001). Evidence for prebudding arrest of ER export in animal cell mitosis and its role in generating Golgi partitioning intermediates. Traffic **2,** 321–335.

Puri, S., and Linstedt, A.D. (2003). Capacity of the Golgi apparatus for biogenesis from the endoplasmic reticulum. Mol. Biol. Cell **14,** 5011–5018.

Ritzenthaler, C., Laporte, C., Gaire, F., Dunoyer, P., Schmitt, C., Duval, S., Piequet, A., Loudes, A.M., Rohfritsch, O., Stussi-Garaud, C., and Pfeiffer, P. (2002b). Grapevine fanleaf virus replication occurs on endoplasmic reticulum-derived membranes. J. Virol. **76,** 8808–8819.

Ritzenthaler, C., Nebenführ, A., Movafeghi, A., Stussi-Garaud, C., Behnia, L., Pimpl, P., Staehelin, L.A., and Robinson, D.G. (2002a). Reevaluation of the effects of brefeldin A on plant cells using tobacco Bright Yellow 2 cells expressing Golgi-targeted green fluorescent protein and COPI antisera. Plant Cell **14,** 237–261.

Rossanese, O.W., Soderholm, J., Bevis, B.J., Sears, I.B., O'Connor, J., Williamson, E.K., and Glick, B.S. (1999). Golgi structure correlates with transitional endoplasmic reticulum organization in *Pichia pastoris* and *Saccharomyces cerevisiae*. J. Cell Biol. **145,** 69–81.

Rust, R.C., Landmann, L., Gosert, R., Tang, B.L., Hong, W., Hauri, H.P., Egger, D., and Bienz, K. (2001). Cellular COPII proteins are involved in production of the vesicles that form the poliovirus replication complex. J. Virol. **75,** 9808–9818.

Seemann, J., Pypaert, M., Taguchi, T., Malsam, J., and Warren, G. (2002). Partitioning of the matrix fraction of the Golgi apparatus during mitosis in animal cells. Science **295,** 848–851.

Segui-Simarro, J.M., Austin II, J.R., White, E., and Staehelin, L.A. (2004). Electron tomographic analysis of somatic cell plate formation

in meristematic cells of Arabidopsis preserved by high-pressure freezing. Plant Cell **16,** 836–856.

Sesso, A., de Faria, F.P., Iwamura, E.S., and Correa, H. (1994). A three-dimensional reconstruction study of the rough ER-Golgi interface in serial thin sections of the pancreatic acinar cell of the rat. J. Cell Sci. **107,** 517–528.

Shorter, J., and Warren, G. (2002). Golgi architecture and inheritance. Annu. Rev. Cell Dev. Biol. **18,** 379–420.

Shugrue, C.A., Kolen, E.R., Peters, H., Czernik, A., Kaiser, C., Matovcik, L., Hubbard, A.L., and Gorelick, F. (1999). Identification of the putative mammalian orthologue of Sec31P, a component of the COPII coat. J. Cell Sci. **112,** 4547–4556.

Siniossoglou, S., Lutzmann, M., Santos-Rosa, H., Leonard, K., Mueller, S., Aebi, U., and Hurt, E. (2000). Structure and assembly of the Nup84p complex. J. Cell Biol. **149,** 41–54.

Soderholm, J., Bhattacharyya, D., Strongin, D., Markovitz, V., Connerly, P.L., Reinke, C.A., and Glick, B.S. (2004). The transitional ER localization mechanism of *Pichia pastoris* Sec12. Dev. Cell **6,** 649–659.

Staehelin, L.A. (1997). The plant ER: A dynamic organelle composed of a large number of discrete functional domains. Plant J. **11,** 1151–1165.

Stephens, D.J. (2003). De novo formation, fusion and fission of mammalian COPII-coated endoplasmic reticulum exit sites. EMBO Rep. **4,** 210–217.

Stephens, D.J., Lin-Marq, N., Pagano, A., Pepperkok, R., and Paccaud, J.P. (2000). COPI-coated ER-to-Golgi transport complexes segregate from COPII in close proximity to ER exit sites. J. Cell Sci. **113,** 2177–2185.

Stephens, D.J., and Pepperkok, R. (2001). Illuminating the secretory pathway: When do we need vesicles? J. Cell Sci. **114,** 1053–1059.

Supek, F., Madden, D.T., Hamamoto, S., Orci, L., and Schekman, R. (2002). Sec16p potentiates the action of COPII proteins to bud transport vesicles. J. Cell Biol. **158,** 1029–1038.

Takeuchi, M., Ueda, T., Sato, K., Abe, H., Nagata, T., and Nakano, A. (2000). A dominant negative mutant of sar1 GTPase inhibits protein transport from the endoplasmic reticulum to the Golgi apparatus in tobacco and Arabidopsis cultured cells. Plant J. **23,** 517–525.

Tang, B.L., Ong, Y.S., Huang, B., Wei, S., Wong, E.T., Qi, R., Horstmann, H., and Hong, W. (2001). A membrane protein enriched in endoplasmic reticulum exit sites interacts with COPII. J. Biol. Chem. **276,** 40008–40017.

Tang, B.L., Zhang, T., Low, D.Y., Wong, E.T., Horstmann, H., and Hong, W. (2000). Mammalian homologues of yeast sec31p. An ubiquitously expressed form is localized to endoplasmic reticulum (ER) exit sites and is essential for ER-Golgi transport. J. Biol. Chem. **275,** 13597–13604.

Vetter, G., Hily, J.M., Klein, E., Schmidlin, L., Haas, M., Merkle, T., and Gilmer, D. (2004). Nucleo-cytoplasmic shuttling of the beet necrotic yellow vein virus RNA-3-encoded p25 protein. J. Gen. Virol. **85,** 2459–2469.

Ward, T.H., and Brandizzi, F. (2004). Dynamics of proteins in Golgi membranes: Comparisons between mammalian and plant cells highlighted by photobleaching techniques. Cell. Mol. Life Sci. **61,** 172–185.

Ward, T.H., Polishchuk, R.S., Caplan, S., Hirschberg, K., and Lippincott-Schwartz, J. (2001). Maintenance of Golgi structure and function depends on the integrity of ER export. J. Cell Biol. **155,** 557–570.

Weissman, J.T., Plutner, H., and Balch, W.E. (2001). The mammalian guanine nucleotide exchange factor mSec12 is essential for activation of the Sar1 GTPase directing endoplasmic reticulum export. Traffic **2,** 465–475.

Wessel, D., and Flügge, U.I. (1984). A method for the quantitative recovery of proteins in dilute solutions in the presence of detergents and lipids. Ann. Biochem. **138,** 141–143.

Zhang, Y.-H., and Robinson, D.G. (1986). The endomembranes of *Chlamydomonas reinhardtii*. A comparison of the wild type with the wall mutants CW2 and CW15. Protoplasma **133,** 186–194.